

DYNAMICAL EVOLUTION OF PLANETESIMALS IN PROTOPLANETARY DISKS.

R. R. RAFIKOV

IAS, Einstein Dr., Princeton, NJ 08540
Draft version August 14, 2018

ABSTRACT

The current picture of terrestrial planet formation relies heavily on our understanding of the dynamical evolution of planetesimals — asteroid-like bodies thought to be planetary building blocks. In this study we investigate the growth of eccentricities and inclinations of planetesimals in spatially homogeneous protoplanetary disks using methods of kinetic theory. Emphasis is put on clarifying the effect of gravitational scattering between planetesimals on the evolution of their random velocities. We explore disks with a realistic mass spectrum of planetesimals evolving in time, similar to that obtained in self-consistent simulations of planetesimal coagulation: distribution scales as a power law of mass for small planetesimals and is supplemented by an extended tail of bodies at large masses representing the ongoing runaway growth in the system. We calculate the behavior of planetesimal random velocities as a function of the planetesimal mass spectrum both analytically and numerically; results obtained by the two approaches agree quite well. Scaling of random velocity with mass can always be represented as a combination of power laws corresponding to different velocity regimes (shear- or dispersion-dominated) of planetesimal gravitational interactions. For different mass spectra we calculate analytically the exponents and time dependent normalizations of these power laws, as well as the positions of the transition regions between different regimes. It is shown that random energy equipartition between different planetesimals can only be achieved in disks with very steep mass distributions (differential surface number density of planetesimals falling off steeper than m^{-4}), or in the runaway tails. In systems with shallow mass spectra (shallower than m^{-3}) random velocities of small planetesimals turn out to be independent of their masses. We also discuss the damping effects of inelastic collisions between planetesimals and of gas drag, and their importance in modifying planetesimal random velocities.

Subject headings: planetary systems: formation — solar system: formation — Kuiper Belt

1. INTRODUCTION.

Gravity-assisted agglomeration of planetesimals in the protoplanetary disks around young stars is a backbone of a currently widely accepted paradigm of terrestrial planet formation, despite many uncertainties in the details of specific processes involved. In many respects our understanding of the planetesimal disk evolution heavily relies on the numerical investigations, and these studies significantly grew in complexity in recent years (Wetherill & Stewart 1989, 1993; Kenyon & Luu 1998, 2002; Inaba et al. 2001). On one hand, the sheer scale of simulated systems has expanded considerably, which was made possible by the increase in computing power; on the other hand, a wider range of concomitant physical phenomena (fragmentation, migration, etc.) can now be routinely followed simultaneously with the evolution of planetesimal mass and velocity distributions.

Unfortunately, very often this complexity creates a problem when one tries to understand a *relative* role of each of the specific processes in shaping the planetesimal mass and velocity spectra. Disentangling the contributions of different physical nature in the results of numerical simulations certainly is a tantalizing task which can often yield very confusing conclusions. Thus it is very important to be able to isolate different physical processes operating in the planetesimal disks and to study their effects on the disk evolution separately. One way to do this is to build simple but realistic models which are easy to

analyze and at the same time are able to grasp the main features of the physics involved. Such approach would grant us good analytical understanding of relevant processes, and we are going to follow this route in our study.

Behavior of planetesimal velocities is one of the crucial ingredients of the terrestrial planet formation picture because of the very important role played by the gravitational focusing (which depends on planetesimal velocities) in assembly of the big bodies in planetesimal disks. The purpose of this paper is to explore the evolution of inclinations and eccentricities (which represent planetesimal random velocities) caused by the mutual gravitational scattering of planetesimals. This is a clean and well-posed problem. The effects of gas drag and inelastic collisions are initially neglected but later on we discuss how their inclusion affects our results. To keep things as clear as possible we have opted not to try coupling self-consistently planetesimal velocity evolution to the evolution of the mass spectrum in this study. Instead, we follow changes of random velocities in a disk with a distribution of planetesimal sizes which evolves in some *prescribed* manner. However simplistic this assumption seems to be, in adopting it we try to use mass spectra which are similar to those produced by self-consistent coagulation simulations, and to study a wide variety of such mass distribution models.

Another argument in favor of this approach is the fact that the dynamical relaxation time in a disk of gravitationally interacting planetesimals is much shorter than the physical collision timescale (characterizing evolution

of the mass spectrum) if relative random velocities of planetesimals are smaller than the escape velocities from their surfaces (which is very often the case). The dynamical evolution of planetesimal disk can then be approximated as that of a system with a quasi-stationary planetesimal mass spectrum. Understanding this problem is a logical step necessary to provide a clearer perspective on how to build a fully self-consistent theory of planet formation.

We describe the statistical approach to the problem of the evolution of planetesimal random velocities in §2. Our model of planetesimal mass spectrum is introduced in §3. In §4 we outline the results for the distribution of planetesimal random velocities vs. planetesimal masses as functions of the input mass distribution and time; we also compare these analytical predictions with numerical results. Table C1 summarizes our major findings in a concise form. In §5 we comment on how gas drag and inelastic collisions between planetesimals can affect planetesimal velocity spectra. We conclude in §6 by the discussion of our results and comparison with previous studies.

2. VELOCITY EVOLUTION EQUATIONS.

When the number of planetesimals in the protoplanetary disk is very large and their masses are not sufficient to induce strong local nonuniformities in the disk (Ida & Makino 1993; Rafikov 2001, 2003b, 2003c), statistical approach and homogeneous “particle in a box” assumption are very helpful in the treatment of planetesimal evolution (Wetherill & Stewart 1989). We assume that planetesimals with mass m have velocity dispersions of eccentricity and inclination $\sigma_e(m, t)$ and $\sigma_i(m, t)$ associated with them. It is natural to characterize planetesimal disk by its mass distribution, and we assume that $N(m, t)dm$ is the *surface number density* of planetesimals with masses between m and $m + dm$.

In studying the dynamics of planetesimal disks we make the following natural assumptions:

- disk is locally homogeneous in radial direction and azimuthally symmetric; it is in Keplerian rotation around central star,
- epicyclic excursions of planetesimals in horizontal and vertical directions are small compared with the distance to the central object,
- planetesimal masses are much smaller than the mass of the central object M_c .

Two important consequences immediately follow from this set of assumptions. First, the gravitational scattering of planetesimals during their encounter can be studied in the framework of Hill approximation (Hénon & Petit 1986; Ida 1990; Rafikov 2003a). In this approach, gravitational interaction between two bodies with masses m and m^* introduces a natural lengthscale — Hill radius¹

$$R_H \equiv a \left(\frac{m + m^*}{M_c} \right)^{1/3}$$

¹ This definition follows original work of Hénon & Petit (1986) and differs from $R_H \equiv a[(m + m^*)/3M_c]^{1/3}$ often used in the literature (e.g. Ida 1990; Stewart and Ida 2000).

$$= 10^{-4} \text{ AU } a_{AU} \left(\frac{m + m^*}{2 \times 10^{21} \text{ g}} \right)^{1/3}, \quad (1)$$

where a is the distance from the central object. Numerical estimate made in (1) assumes $M_c = M_\odot$ and $a_{AU} \equiv a/(1 \text{ AU})$, and is intended to illustrate that typically $R_H \ll a$. Hill approximation yields two significant simplifications:

- The outcome of the interactions between two bodies depends only on their *relative* velocities and distances.
- If all relative distances are scaled by R_H and relative velocities of interacting bodies are scaled by ΩR_H , then the outcome of the gravitational scattering depends only on the initial values of scaled relative quantities.

Second, numerical studies (Greenzweig & Lissauer 1992; Ida & Makino 1992) have demonstrated that in homogeneous planetesimal disks the distribution function $\psi(e, i)$ of absolute values of planetesimal eccentricities e and inclinations i is well represented by the Rayleigh distribution:

$$\psi(e, i)dedi = \frac{edeidi}{\sigma_e^2\sigma_i^2} \exp \left[-\frac{e^2}{2\sigma_e^2} - \frac{i^2}{2\sigma_i^2} \right], \quad (2)$$

where σ_e and σ_i are the aforementioned dispersions of eccentricity and inclination. It also follows from azimuthal symmetry that horizontal and vertical epicyclic phases τ and ω are distributed uniformly in the interval $(0, 2\pi)$. These facts have important ramifications as we demonstrate below.

Let’s consider the gravitational interaction of two planetesimal populations: one with mass m and eccentricity and inclination dispersions σ_e and σ_i and the other with mass m^* and dispersions σ_e^* and σ_i^* . When the velocity² distribution function of planetesimals has the form (2) it can be shown (Rafikov 2003a) that the evolution of σ_e and σ_i due to the gravitational interaction with population of mass m^* proceeds according to

$$\begin{aligned} \frac{\partial \sigma_e^2}{\partial t} &= |A|N^*a^2 \left(\frac{m + m^*}{M_c} \right)^{4/3} \frac{m^*}{m + m^*} \\ &\times \left[\frac{m^*}{m + m^*} H_1 + 2 \frac{\sigma_e^2}{\sigma_e^2 + \sigma_e^{*2}} H_2 \right], \\ \frac{\partial \sigma_i^2}{\partial t} &= |A|N^*a^2 \left(\frac{m + m^*}{M_c} \right)^{4/3} \frac{m^*}{m + m^*} \\ &\times \left[\frac{m^*}{m + m^*} K_1 + 2 \frac{\sigma_i^2}{\sigma_i^2 + \sigma_i^{*2}} K_2 \right], \end{aligned} \quad (3)$$

where N^* is the surface number density of planetesimals of mass m^* , and $A = -(r/2)d\Omega/dr$ is a measure of shear in the disk [in Keplerian disks $A = -(3/4)\Omega$]. Scattering coefficients $H_{1,2}$ are defined as

$$\begin{aligned} H_1 &= H_1(\tilde{\sigma}_{er}, \tilde{\sigma}_{ir}) \\ &= \int d\tilde{\mathbf{e}}_r d\tilde{\mathbf{i}}_r \tilde{\psi}_r(\tilde{\mathbf{e}}_r, \tilde{\mathbf{i}}_r) \int_{-\infty}^{\infty} d\tilde{h} |\tilde{h}| (\Delta\tilde{\mathbf{e}}_{sc})^2, \end{aligned}$$

² Throughout the paper we often refer to eccentricities and inclinations of planetesimals as their random velocities.

$$\begin{aligned}
H_2 &= H_2(\tilde{\sigma}_{er}, \tilde{\sigma}_{ir}) \\
&= \int d\tilde{\mathbf{e}}_r d\tilde{\mathbf{i}}_r \tilde{\psi}_r(\tilde{\mathbf{e}}_r, \tilde{\mathbf{i}}_r) \int_{-\infty}^{\infty} d\tilde{h} |\tilde{h}| |(\tilde{\mathbf{e}}_r \cdot \Delta\tilde{\mathbf{e}}_{sc}), \quad (4)
\end{aligned}$$

where $\tilde{\sigma}_{er,ir} = (\sigma_{e,i}^2 + \sigma_{e,i}^{*2})^{1/2} a/R_H$ are the dispersions of relative eccentricity and inclination normalized in Hill coordinates [see (1)], \tilde{h} is a semimajor axes difference of interacting bodies scaled by R_H , and $\tilde{\mathbf{e}}_r, \tilde{\mathbf{i}}_r$ are the relative eccentricity and inclination *vectors* in Hill units (Goldreich & Tremaine 1980; Ida 1990). Function $\Delta\tilde{\mathbf{e}}_{sc}$ represents a change of $\tilde{\mathbf{e}}_r$ produced in the course of scattering, which is a function of not only absolute values of \tilde{e}_r, \tilde{i}_r , and \tilde{h} , but also of the relative epicyclic phases (for which reason we use vector eccentricities and inclinations here). The distribution function of relative eccentricities and inclinations of planetesimals $\tilde{\psi}_r(\tilde{\mathbf{e}}_r, \tilde{\mathbf{i}}_r)$ is analogous in its functional form to (2), but with $\sigma_{e,i}$ replaced by *relative* velocity dispersions $\tilde{\sigma}_{er,ir}$. Expressions analogous to (4) can be written down also for inclination scattering coefficients K_1 and K_2 . Note that the only assumption used in deriving (3) is that of the specific form (2) of the distribution function of planetesimal eccentricities and inclinations (Rafikov 2003a).

Equations (3) describe dynamical evolution driven only by gravitational scattering of planetesimals, implicitly assuming that they are point masses. Physical size of planetesimal $r_p \approx 3 \times 10^{-7}$ AU ($m/(10^{21} \text{ g})^{1/3}$ (for physical density 3 g cm^{-3}) is very small compared to the corresponding Hill radius (1), which often justifies the neglect of physical collisions between planetesimals. However, at high relative velocities — higher than the escape speed from planetesimal surfaces — one can no longer disregard highly inelastic physical collisions which strongly damp planetesimal random motions. In this study we proceed by assuming first that velocities of planetesimals are below their escape velocities, and then discussing in §5 how abandoning this assumption affects our conclusions.

Equation (3) and definitions (4) have been previously derived by other authors in a slightly different form (Wetherill & Stewart 1988; Ida 1990; Tanaka & Ida 1996; Stewart & Ida 2000):

$$\begin{aligned}
\frac{\partial \sigma_e^2}{\partial t} &= |A| N^* a^2 \left(\frac{m+m^*}{M_c} \right)^{4/3} \frac{m^*}{m+m^*} \\
&\times \left[\frac{m^*}{m+m^*} (H_1 + 2H_2) + 2 \frac{m}{m+m^*} \frac{\sigma_e^2}{\sigma_e^2 + \sigma_e^{*2}} H_2 \right. \\
&\left. - 2 \frac{m^*}{m+m^*} \frac{\sigma_e^{*2}}{\sigma_e^2 + \sigma_e^{*2}} H_2 \right]. \quad (5)
\end{aligned}$$

In this form the first term in brackets on the r.h.s. describes the so-called *viscous stirring* which is proportional to the phase space average of $\Delta(\mathbf{e}_r^2)$ (see definitions of H_1 and H_2). Depending on $\tilde{\sigma}_{er}$ and $\tilde{\sigma}_{ir}$ it can be either positive or negative. Second term represents the phenomenon of *dynamical friction* well known from galactic dynamics. In the limit $m \gg m^*$ its contribution is proportional to the mass of particle under consideration and to the surface mass density of field particles, but is independent of individual masses of field particles (cf. Binney & Tremaine 1987). This term is negative since it represents the gravitational interaction of a moving body with

the wake of field particles formed *behind* it as a result of gravitational focusing; thus $H_2 < 0$ and $K_2 < 0$. Finally, the third term describes the increase of random velocities of a particular body at the expense of random motion of field planetesimals it interacts with. This effect is analogous to the first order Fermi mechanism of the cosmic ray acceleration via scattering of energetic particles by randomly moving magnetic field inhomogeneities (Fermi 1949). Note that in previous studies of planetesimal scattering it is the combination of the second and third terms on the r.h.s. of (5) that is called the dynamical friction (Stewart & Wetherill 1988; Ida 1990). The combined effect of these two terms is to drive planetesimal system to equipartition of random energy between planetesimals of different mass (which would be realized in the absence of viscous stirring).

In this work we analyze planetesimal velocity evolution with the aid of equation (3). We call the first (positive) term on its r.h.s. *gravitational stirring* or *heating* (different from viscous stirring), while second (negative) term is called *gravitational friction* or *cooling* (different from dynamical friction³). In this sense terms “stirring” and “friction” are only used to describe positive and negative contributions to the growth rate of planetesimals random motion. Use of equations (3) rather than (5) has two obvious advantages: (1) gravitational stirring and friction have different dependences on $m^*/(m+m^*)$ which considerably simplifies analysis of velocity evolution equations, and (2) stirring and friction terms have definite signs (unlike viscous stirring and dynamical friction used in previous studies of planetesimal dynamics).

Gravitational scattering of planetesimals can proceed in two rather different velocity regimes, shear-dominated and dispersion-dominated. The former one is realized when $\sigma_{e,i}^2 + \sigma_{e,i}^{*2} \ll (R_H/a)^2$, while the latter holds when $\sigma_{e,i}^2 + \sigma_{e,i}^{*2} \gg (R_H/a)^2$. Analytical arguments and numerical calculations demonstrate that in the dispersion-dominated regime σ_e and σ_i are of the same order and evolve in a similar fashion (e.g. Ida 1990; Stewart & Ida 2000). This happens because scattering in this regime has a three-dimensional character making different components of velocity ellipsoid comparable to each other. Thus, rough idea of the dynamical evolution in this case can be obtained by studying only one of the equations (3). Moreover, the behavior of the scattering coefficients in the dispersion-dominated regime can be calculated analytically as a function of $\tilde{\sigma}_{er}$ and $\tilde{\sigma}_{ir}$ in two-body approximation (Stewart & Wetherill 1988; Tanaka & Ida 1996), and one finds that

$$\begin{aligned}
\left\{ \begin{array}{l} H_1 \\ K_1 \end{array} \right\} &= \left\{ \begin{array}{l} A_1 (\tilde{\sigma}_{ir}/\tilde{\sigma}_{er}) \\ C_1 (\tilde{\sigma}_{ir}/\tilde{\sigma}_{er}) \end{array} \right\} \frac{\ln \Lambda}{\tilde{\sigma}_{er}^2}, \\
\left\{ \begin{array}{l} H_2 \\ K_2 \end{array} \right\} &= - \left\{ \begin{array}{l} A_2 (\tilde{\sigma}_{ir}/\tilde{\sigma}_{er}) \\ C_2 (\tilde{\sigma}_{ir}/\tilde{\sigma}_{er}) \end{array} \right\} \frac{\ln \Lambda}{\tilde{\sigma}_{er}^2}, \quad (6)
\end{aligned}$$

where $A_{1,2}, C_{1,2}$ are positive functions of inclination to eccentricity ratio $\tilde{\sigma}_{ir}/\tilde{\sigma}_{er}$, and $\ln \Lambda$ is a Coulomb logarithm (Binney & Tremaine 1987), which in our case can be represented as (Rafikov 2003a)

$$\Lambda \approx a_1 \tilde{\sigma}_{ir} (\tilde{\sigma}_{er}^2 + a_2 \tilde{\sigma}_{ir}^2), \quad (7)$$

³ I am grateful to Peter Goldreich and Re'em Sari for pointing this out to me.

with $a_{1,2}$ being some constants. Explicit analytical expressions for coefficients $A_{1,2}, C_{1,2}$ have been derived by Stewart & Ida (2000). One can deduce a specific useful property of these functions by considering a single-mass planetesimal population: in dispersion-dominated regime the distribution of random energy between the vertical and horizontal motions tends to reach a quasi-equilibrium state (see e.g. Ida & Makino 1992). Then the ratio σ_{ir}/σ_{er} is almost constant and both σ_{er} and σ_{ir} grow with time, meaning that [see (3) & (6)]

$$A_1 > 2A_2, \quad C_1 > 2C_2. \quad (8)$$

This property will be used later in §4 & C.

In the shear-dominated regime σ_e and σ_i evolve along different routes: eccentricity is excited much stronger than inclination because in this regime disk is geometrically thin and forcing in the plane of the disk is stronger than in perpendicular direction. Eccentricity evolution is also quite rapid in this case because of the vigorous scattering (relative horizontal velocity increases by $\sim \Omega R_H$ in each synodic passage of two bodies initially separated by $\sim R_H$ in semimajor axes). Simple reasoning confirmed by numerical experiments suggests the following behavior of scattering coefficients in the shear-dominated regime:

$$H_1(\tilde{\sigma}_{er}, \tilde{\sigma}_{ir}) \approx B_1, \quad H_2(\tilde{\sigma}_{er}, \tilde{\sigma}_{ir}) \approx -B_2 \tilde{\sigma}_{er}^2, \\ K_1(\tilde{\sigma}_{er}, \tilde{\sigma}_{ir}) \approx D_1 \tilde{\sigma}_{ir}^2, \quad K_2(\tilde{\sigma}_{er}, \tilde{\sigma}_{ir}) \approx -D_2 \tilde{\sigma}_{ir}^2, \quad (9)$$

where $B_{1,2}, D_{1,2}$ are some positive constants, which can be fixed using numerical orbit integrations, see Appendix A. Simple qualitative derivation of (6) and (9) can be found in Ida & Makino (1993) and Rafikov (2003c).

For further convenience, we now reduce evolution equations to a dimensionless form. We relate planetesimal masses to the smallest planetesimal mass⁴ m_0 by using dimensionless quantity $x = m/m_0$. Instead of $N(m)$ we introduce dimensionless mass distribution function $f(x)$ such that

$$N(m) = \frac{\Sigma_p}{m_0^2} f(x) \quad \text{and} \quad N(m)dm = \frac{\Sigma_p}{m_0} f(x)dx, \quad (10)$$

where Σ_p is the total mass surface density of planetesimals in the disk, which is a conserved quantity. We also rescale eccentricity and inclination dispersions:

$$s = \sigma_e \left(\frac{m_0}{M_c} \right)^{-1/3}, \quad s_z = \sigma_i \left(\frac{m_0}{M_c} \right)^{-1/3}. \quad (11)$$

This is equivalent to rescaling all distances by Hill radius of smallest planetesimals. In this notation the boundary between the shear- and dispersion-dominated regimes is given by conditions

$$s^2 + s^{*2} \approx (x + x^*)^{2/3}, \quad s_z^2 + s_z^{*2} \approx (x + x^*)^{2/3}. \quad (12)$$

We also introduce dimensionless time τ by

$$\tau = \frac{t}{t_0}, \quad \text{where} \quad t_0 = |A|^{-1} \frac{m_0}{\Sigma_p a^2} \left(\frac{m_0}{M_c} \right)^{-2/3} \quad (13)$$

⁴ Protoplanetary disks should contain planetesimals of different sizes but we assume that bodies lighter than m_0 are not important for the disk evolution. In the case considered here the choice of m_0 is dictated by the mass at which distribution would depart from the given power law form towards shallower scaling with mass (see also §4.1.1).

is a timescale for the stirring of planetesimal disk composed of bodies of mass m_0 only, on the boundary between the shear- and dispersion-dominated regimes. Numerically, for $M_c = M_\odot$ one finds that

$$t_0 \approx 16 \text{ yr } a_{AU} \left(\frac{10 \text{ g cm}^{-2}}{\Sigma_{p0}} \right) \left(\frac{m_0}{10^{21} \text{ g}} \right)^{1/3}, \quad (14)$$

where we assumed that $\Sigma_p(a) = \Sigma_{p0} a_{AU}^{-3/2}$ (Hayashi 1981). Dynamical timescale is rather short when $s, s_z \sim 1$, but it grows very rapidly as epicyclic velocities of planetesimals increase ($t \sim t_0 s^4$ in the dispersion-dominated regime).

Random velocities of planetesimals of mass x evolve due to the interaction with all other bodies spanning the whole mass spectrum. Using our dimensionless notation we can rewrite equations (3), (6), & (9) in the following general form:

$$\frac{\partial s^2}{\partial \tau} = \int_1^\infty dx^* f(x^*) x^* (x + x^*)^{1/3} \\ \times \left[\frac{x^*}{x + x^*} H_1 + 2 \frac{s^2}{s^2 + s^{*2}} H_2 \right], \quad (15)$$

$$\frac{\partial s_z^2}{\partial \tau} = \int_1^\infty dx^* f(x^*) x^* (x + x^*)^{1/3} \\ \times \left[\frac{x^*}{x + x^*} K_1 + 2 \frac{s_z^2}{s_z^2 + s_z^{*2}} K_2 \right], \quad (16)$$

where $s \equiv s(x), s^* \equiv s(x^*)$ and similarly for s_z, s_z^* ; in the shear-dominated regime [$s^2 + s^{*2}, s_z^2 + s_z^{*2} \ll (x + x^*)^{2/3}$]

$$H_1 \approx C_1, \quad H_2 \approx -C_2 \frac{s^2 + s^{*2}}{(x + x^*)^{2/3}}, \\ K_1 \approx D_1 \frac{s_z^2 + s_z^{*2}}{(x + x^*)^{2/3}}, \quad K_2 \approx -D_2 \frac{s_z^2 + s_z^{*2}}{(x + x^*)^{2/3}}, \quad (17)$$

and in the dispersion-dominated regime [$s^2 + s^{*2}, s_z^2 + s_z^{*2} \gg (x + x^*)^{2/3}$]

$$\left(\frac{H_1}{K_1} \right) = \left(\frac{A_1}{B_1} \right) \frac{(x + x^*)^{2/3}}{s^2 + s^{*2}} \ln \Lambda, \\ \left(\frac{H_2}{K_2} \right) = - \left(\frac{A_2}{B_2} \right) \frac{(x + x^*)^{2/3}}{s^2 + s^{*2}} \ln \Lambda. \quad (18)$$

We explore this system in §4 using two approaches: asymptotic analysis utilizing analytical methods, and direct numerical calculation of velocity evolution.

3. MASS SPECTRUM.

Starting from (15)-(18) one would like to obtain the behavior of s and s_z as functions of x and τ , given some planetesimal mass spectrum $f(x)$ as an input. In general, to do this one has to evolve equations (16)-(18) numerically. However, it is usually true that the planetesimal size distribution spans many orders of magnitude in mass; thus one would expect that some general predictions can be made analytically about the asymptotic properties of planetesimal velocity spectrum.

In this study we assume that planetesimal mass distribution has a ‘‘self-similar’’ form; specifically we take

$$f(x, \tau) = \psi(\tau) \varphi \left(\frac{x}{x_c(\tau)} \right), \quad (19)$$

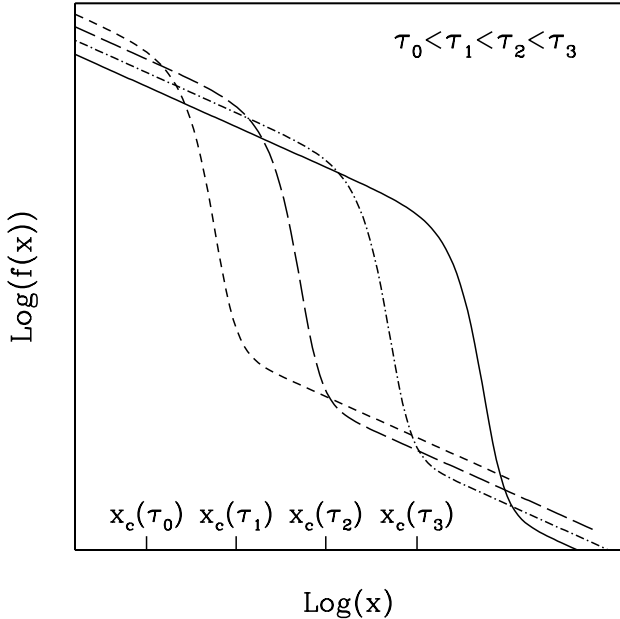


FIG. 1.— Schematic representation of the shape of planetesimal mass spectrum and its evolution in time. Mass distribution has a power law form exponentially cut off at $x_c(\tau)$ with a tail of runaway bodies for $x \gg x_c(\tau)$.

where $x_c(\tau) \gg 1$ is some fiducial planetesimal mass which steadily grows in time as a result of coagulation, $\psi(\tau)$ is a temporal modulation, and function φ represents a self-similar shape of the mass spectrum. We also assume in this study that asymptotically

$$\varphi(y) \sim \begin{cases} y^{-\alpha}, & y \ll 1, \\ \exp(-y), & y \gg 1, \end{cases} \quad (20)$$

where $\alpha > 0$. Such scaling behavior is often found in coagulation simulations. We will see in §4 that for clarifying the asymptotic properties of planetesimal velocity spectrum it is enough to know only the asymptotic behavior of $\varphi(y)$ and not its exact shape. Moreover, in §6 we demonstrate how our results for power-law size distributions can be generalized for other mass spectra.

Normalization $\psi(\tau)$ is not an independent function. It is related to $x_c(\tau)$ because of the conservation of the total (dimensionless) planetesimal surface density

$$M_1 \equiv \int_1^{\infty} x f(x) dx. \quad (21)$$

Taking this constraint into account one finds that

$$\psi(\tau) = \begin{cases} x_c^{-2}(\tau), & \alpha < 2, \\ x_c^{-\alpha}(\tau), & \alpha > 2. \end{cases} \quad (22)$$

In the case $\alpha > 2$ mass spectrum behaves as $f(x, \tau) = x^{-\alpha}$ for $x \ll x_c(\tau)$; only the position of the high mass cutoff $x_c(\tau)$ shifts towards higher and higher masses with time.

We define $M_\nu(\tau)$ to be the ν -th order moment of the mass distribution:

$$M_\nu(\tau) \equiv \int_1^{\infty} (x^*)^\nu f(x^*, \tau) dx^*. \quad (23)$$

Integral in (23) is dominated by the upper end of the power-law part of the mass spectrum (i.e. by $x^* \sim x_c$) if $\nu > \alpha - 1$; in this case we can write [using (19)]

$$\begin{aligned} M_\nu(\tau) &= \tilde{M}_\nu [x_c(\tau)]^{\nu+1} \psi(\tau) \\ &= \tilde{M}_\nu \begin{cases} x_c^{\nu-1}, & \alpha < 2, \\ x_c^{\nu+1-\alpha}, & \alpha > 2, \end{cases}, \quad \tilde{M}_\nu \equiv \int_0^{\infty} y^\nu \varphi(y) dy, \end{aligned} \quad (24)$$

where \tilde{M}_ν — *reduced moment* of order ν — is a time-independent constant for a given mass distribution.

One of the interesting features exhibited by self-consistent coagulation simulations is the development of the tail of high mass bodies beyond the cutoff of the bulk distribution of planetesimals (Wetherill & Stewart 1989; Inaba et al. 2001). This is interpreted as the manifestation of the *runaway* phenomenon taking place in a coagulating system. To explore the possibility of the runaway scenario we add to the mass spectrum (20) a tail of high mass planetesimals extending beyond the exponential cutoff x_c (see Appendix A). In doing this we always make sure that runaway tail contains a negligible part of the system’s mass and does not affect its dynamical state (i.e. stirring and friction caused by these high mass planetesimals are small) which is true if biggest bodies are not too massive (Rafikov 2003c). Under these assumptions the explicit functional form of the runaway tail is completely unimportant. Throughout this study, we use the term “planetesimals” for bodies belonging to the power-law part of the spectrum ($x \lesssim x_c$), and “massive” or “runaway” bodies to denote the constituents of the tail ($x \gg x_c$).

We do not restrict the variety of possible functional dependences of x_c on time τ . It will turn out that all our results can be expressed as some functions of x_c which leads to the time-dependence of planetesimal velocities in a very general form. In some cases it will be important that $x_c(\tau)$ does not grow too fast, which, however, we believe is a fairly weak constraint (see discussion in §4.1.2).

4. VELOCITY SCALING LAWS.

To facilitate our treatment of planetesimal velocities we introduce a set of simplifications into our consideration:

- We split mass spectrum into several regions, such that in each of them planetesimal interactions can be considered as dominated by a single dynamical regime (shear-dominated or dispersion-dominated). Transitions between such regions are not considered but in principle might be treated by interpolation.
- When studying the dispersion-dominated regime we neglect the difference between the vertical and horizontal velocity dispersions, and treat them by a single equation. We also set Coulomb logarithm equal to constant, because of its rather weak dependence on s, s_z or x .

The validity and impact of these assumptions on the velocity spectrum are further checked using numerical techniques. Since we are mostly interested in qualitative behavior of solutions, we do not expect numerical constants

to be correctly reproduced by our analysis; they can be trivially fixed using numerical calculations.

Mass distributions are parametrized by the value of power law exponent α [see (20)]. We split our investigation according to the value of α into 3 cases: *shallow* mass spectrum, $\alpha < 2$, *intermediate* mass spectrum, $2 < \alpha < 3$, and *steep* spectrum, $\alpha > 3$ (this regime splits into two more important subcases, see §4.3). Note that for the sake of avoiding additional complications we do not consider borderline cases $\alpha = 2, 3$; they can be easily studied in the framework of our approach if the need arises.

In our analytical work planetesimals are started with large enough s and s_z so that they interact with each other in the dispersion-dominated regime. We then also assume that planetesimals with masses $x \lesssim x_c(\tau)$ (containing most of the mass) stay in the dispersion-dominated regime w.r.t. each other also at later time, i.e.

$$s(x, \tau), s_z(x, \tau) \gg x^{1/3} \quad \text{for } x \lesssim x_c(\tau). \quad (25)$$

This is a reasonable assumption for all mass spectra at the beginning of evolution, although for steep size distributions it may break down when maximum planetesimal mass becomes very large (see §4.3).

4.1. Shallow mass spectrum.

Planetesimal mass distributions shallower than m^{-2} result from coagulation of high-velocity planetesimals, when gravitational focusing is unimportant and collision rate is determined by geometrical cross-section of colliding bodies (Wetherill & Stewart 1993; Kenyon & Luu 1998). It is worth remembering however that in highly dynamically excited disks (1) energy dissipation in inelastic collisions must be important, see §5, and (2) planetesimal fragmentation cannot be ignored. Despite that, the case of shallow mass spectrum is interesting because it facilitates understanding of the disks with other planetesimal size distributions.

4.1.1. Velocities of planetesimals.

We start by considering planetesimals, $x \lesssim x_c(\tau)$ — part of the size distribution containing most of the mass. Regarding them as interacting in the dispersion-dominated regime [i.e. the condition (25) is fulfilled] we may write using (16) & (18) that

$$\begin{aligned} \frac{\partial s^2}{\partial \tau} &= \int_1^\infty dx^* f(x^*) \frac{x^*(x+x^*)}{s^2+s^{*2}} \\ &\times \left[\frac{x^*}{x+x^*} A_1 - 2 \frac{s^2}{s^2+s^{*2}} A_2 \right] \end{aligned} \quad (26)$$

for $x \ll x_c(\tau)$. Since we use a single equation to describe the evolution of both s and s_z , the values of constants $A_{1,2}$ are not well defined but this is not important for deriving general properties of the velocity spectrum.

We can represent (26) asymptotically in the following form:

$$\begin{aligned} \frac{\partial s^2}{\partial \tau} &\approx A_1 \int_1^{\tilde{x}} dx^* \frac{x^{*2} f(x^*)}{s^2+s^{*2}} - 2A_2 s^2 x \int_1^{\tilde{x}} dx^* \frac{x^* f(x^*)}{(s^2+s^{*2})^2} \\ &+ \int_{\tilde{x}}^\infty dx^* \frac{x^{*2} f(x^*)}{s^2+s^{*2}} \left[A_1 - 2 \frac{s^2}{s^2+s^{*2}} A_2 \right]. \end{aligned} \quad (27)$$

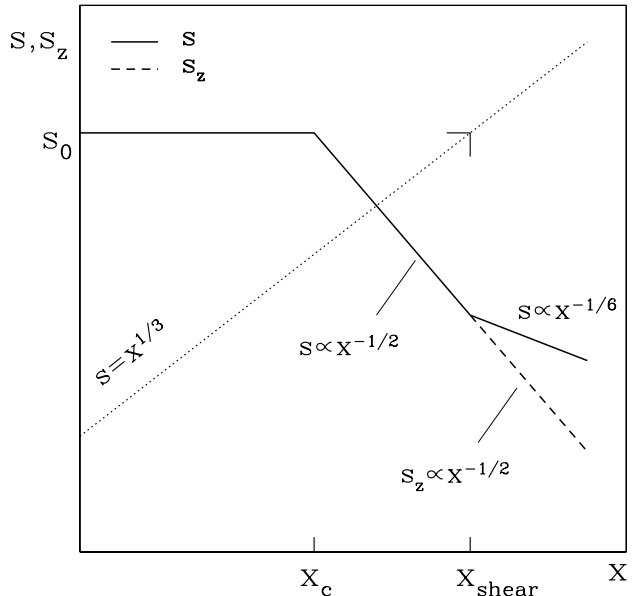


FIG. 2.— Sketch of the behavior of the scaled planetesimal eccentricity and inclination $s = \sigma_e a/r_H$ and $s_z = \sigma_i a/r_H$ as functions of their dimensionless mass $x = m/m_0$, predicted by asymptotic analysis of §4.1. Solid line displays $s(x)$ while dashed line is for $s_z(x)$ (for $x < x_{shear}$ their behaviors are the same). Dotted line delineates shear- and dispersion-dominated regimes of planetesimal interaction with bodies of comparable mass. The rest of notation and theoretical predictions for the temporal behavior of $s(x)$ and $s_z(x)$ can be found in the text.

The first two terms on the r.h.s. represent correspondingly the gravitational stirring and friction by bodies smaller than x . The last term is responsible for the combined effect of stirring and friction produced by bodies bigger than x . From this equation it is easy to see that $s(\tau)$ independent of x is a legitimate solution of (27) in the case $\alpha < 2$. Indeed, assuming s to be independent of x we find that all integrals over x^* in (27) are dominated by their upper limits when mass spectrum is shallow. Using (19)-(24) we can estimate that

$$\begin{aligned} \frac{\partial s^2}{\partial \tau} &\approx A_1 \frac{x_c}{2s^2} \left(\frac{x}{x_c} \right)^{3-\alpha} - 2A_2 \frac{x_c}{4s^2} \left(\frac{x}{x_c} \right)^{3-\alpha} \\ &+ (A_1 - A_2) \frac{M_2(\tau)}{2s^2}. \end{aligned} \quad (28)$$

Note that in deriving this expression we have extended the integration range of the last term in (27) from 1 to infinity (not from $\sim x$). This is legitimate because this integral is dominated by the contribution coming from $\sim x_c \gg x$ and, thus, adding interval from 1 to $\sim x$ to integration range would introduce only a subdominant contribution to the final answer. Clearly, two first terms in (28) are negligible compared to the third one for $x \ll x_c$, and third term is positive [see (8)] and independent of x , meaning that $s(\tau)$ is also independent of mass, in accord with our assumption. One can then easily find that⁵ [dropping constant factors $A_{1,2}$ but bearing in mind

⁵ Throughout the paper we imply by s_0 the velocity dispersion of smallest planetesimals and s_0 is different for different mass spectra, see (40) and (53) below.

condition (8)]

$$s(x, \tau) \approx s_0 \equiv \left[\int_0^\tau M_2(\tau') d\tau' \right]^{1/4} \\ = \left[\tilde{M}_2 \int_0^\tau x_c(\tau') d\tau' \right]^{1/4}, \quad \alpha < 2, \quad x \lesssim x_c \quad (29)$$

[if $s(x, \tau) \gg s(x, 0)$]. The second equality holds only for $\alpha < 2$, according to (22) & (24). Thus, in the case of mass spectrum shallower than x^{-2} random velocities are independent of planetesimal masses and uniformly grow with time. Both gravitational stirring and friction are dominated by biggest planetesimals ($x \sim x_c$), with stirring being more important; friction by small bodies is completely negligible and energy equipartition between planetesimals of different mass is not reached. For this reason, planetesimal velocity expressed in physical units using (11), (13), & (29) is independent of the choice of m_0 . A schematic representation of velocity spectrum for the shallow mass distribution is displayed in Figure 2.

4.1.2. Velocities of runaway bodies.

Now we turn our attention to the runaway bodies, $x \gg x_c$. By assumption, this tail contains so little mass, that it cannot affect velocities not only of planetesimals but also of runaway bodies themselves.

Because of our assumption of the dispersion-dominated interaction between all planetesimals with $x \lesssim x_c$ it is natural to expect that at least those runaway bodies which are not too heavy still experience dispersion-dominated scattering by planetesimals with masses $\lesssim x_c$. Assuming that the velocity dispersion of these runaway bodies is much smaller than that of the bulk of planetesimals — natural consequence of the tendency to equipartition of random epicyclic energy between bodies of different mass — we can rewrite (26) as

$$\frac{\partial s^2}{\partial \tau} \approx A_1 \int_1^\infty dx^* \frac{x^{*2} f(x^*)}{s^{*2}} - 2A_2 s^2 x \int_1^\infty dx^* \frac{x^* f(x^*)}{s^{*4}} \quad (30)$$

Although the integration range of all terms in the r.h.s. is extended to infinity, the exponential cutoff of $f(x)$ at $\sim x_c$ effectively restricts the integration range to be from 1 to $\sim x_c$.

One can easily see that $s(x, \tau) = \text{const}(x)$ cannot be a solution of (30) because dynamical friction is too strong. Indeed, if we were to assume the opposite, we would find that $s(x, \tau)$ is still given by (29). However, direct substitution of (29) into (30) shows that the gravitational friction term exceeds other contributions for $x \gtrsim x_c$. This might tempt one to suggest that heating (first) term in r.h.s. (30) should be neglected compared to the friction (second) term. In this case one would find that $s(x, \tau)$ exponentially decays in time and very soon heating term becomes the dominant one, contrary to initial assumption. These results suggest the only remaining possibility — that heating of massive bodies by planetesimals almost exactly balances friction by planetesimals, and minute difference between them is accounted for by the time dependence of $s(x, \tau)$ embodied in the l.h.s. of (30).

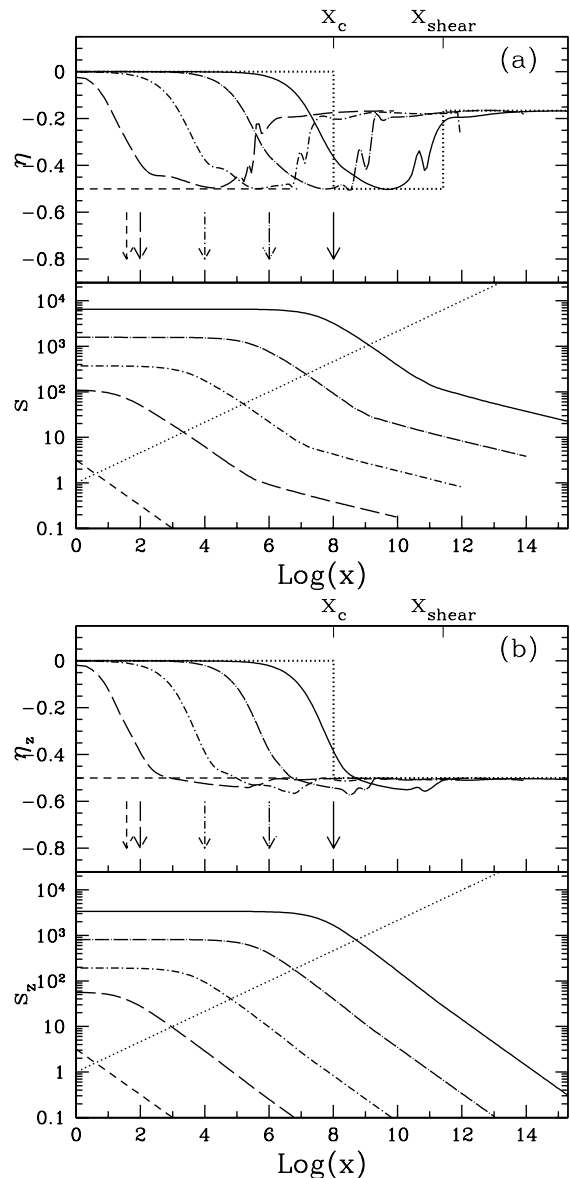


FIG. 3.— Numerical results in the case of $\alpha = 1.5$ for (a) eccentricity dispersion (dimensionless) s and (b) inclination dispersion s_z . In the bottom panels the velocity spectrum is plotted as a function of dimensionless mass x , while in the top panels the power law index $\eta = d \ln s / d \ln x$ of the spectrum is displayed. Different curves correspond to increasing values of maximum planetesimal mass x_c (and, consequently, time) indicated by arrows of corresponding line type on the upper panels. Dotted line in the lower panels is $s = x^{1/3}$ (boundary between different velocity regimes). Dotted curve in the upper panels is the theoretical prediction for the run of the spectral index η corresponding to the largest x_c displayed (for which numerical result is always shown by thick solid line). These results are to be compared with theoretical predictions shown in Figure 2.

Given that this assumption is correct we immediately find that

$$s(x, \tau) \approx \frac{1}{\sqrt{x}} \left[\int_1^\infty dx^* \frac{x^{*2} f(x^*)}{s^{*2}} \right]^{1/2} \left[\int_1^\infty dx^* \frac{x^* f(x^*)}{s^{*4}} \right]^{-1/2} \quad (31)$$

It is easy to see that scaling $s \propto x^{-1/2}$ follows di-

rectly from assuming that (1) the interaction is in the dispersion-dominated regime, and (2) heating of runaway bodies by planetesimals is balanced by friction also due to planetesimals. This specific result is completely independent of the mass or velocity spectra of small bodies. We will highlight this again when we obtain similar results for intermediate and steep mass spectra in §4.2.2 and §C.2. For a specific case $\alpha < 2$ considered in this section $s^* = s_0(\tau)$ and one finds that

$$\begin{aligned} s(x, \tau) &\approx \frac{s_0(\tau)}{\sqrt{x}} \left[\frac{M_2(\tau)}{M_1} \right]^{1/2} \\ &= s_0 \left(\frac{x_c}{x} \right)^{1/2} \left(\frac{\tilde{M}_2}{M_1} \right)^{1/2}, \quad x_c \lesssim x \lesssim x_{shear} \quad (32) \end{aligned}$$

[x_{shear} is defined below in equation (33)]. At $x \sim x_c$ this formula is consistent with s_0 — extrapolation of small mass result (29) up to $x \sim x_c$.

Time dependence enters (32) eventually through $x_c(\tau)$. Thus, it is the behavior of $x_c(\tau)$ that determines $\partial s^2 / \partial \tau$ in (30). The timescale on which x_c varies is usually much longer than the dynamical relaxation time of the system, thus one would expect l.h.s. of (30) to be small in accordance with the assumptions which led to (31). The requirement of the negligible effect of time derivatives in situations like the one described here is the only constraint which must be imposed on the possible behavior of $x_c(\tau)$.

As we consider even bigger x we find that at some mass runaway bodies start interacting with bodies of similar mass in the shear-dominated regime; this happens when $x^{1/3} \sim s_0(x_c/x)^{1/2}$, or $x \sim x_c(s_0/x_c^{1/3})^{6/5}$. This, however does not affect the dynamics of these bodies, because by our assumption runaway tail contains too little mass to dynamically affect its own constituents. It is only after the runaway bodies start interacting in the shear-dominated regime with *planetesimals* (i.e. bodies lighter than x_c), that the velocity evolution of the tail gets affected. In our case this clearly happens when $x^{1/3} \sim s_0(\tau)$. Thus, runaway bodies with masses

$$x \gtrsim x_{shear} \equiv s_0^3 \quad (33)$$

interact with all planetesimals in the shear-dominated regime.

As mentioned in §2, in the shear-dominated case eccentricities and inclinations may no longer evolve along similar routes and we have to consider them separately. Using (16) & (17) we write

$$\begin{aligned} \frac{\partial s^2}{\partial \tau} &= \int_1^\infty dx^* f(x^*) x^* (x + x^*)^{1/3} \\ &\times \left[C_1 \frac{x^*}{x + x^*} - 2C_2 \frac{s^2}{(x + x^*)^{2/3}} \right], \quad (34) \end{aligned}$$

$$\begin{aligned} \frac{\partial s_z^2}{\partial \tau} &= \int_1^\infty dx^* f(x^*) x^* \frac{s_z^2 + s_z^{*2}}{(x + x^*)^{1/3}} \\ &\times \left[D_1 \frac{x^*}{x + x^*} - 2D_2 \frac{s_z^2}{s_z^2 + s_z^{*2}} \right]. \quad (35) \end{aligned}$$

Assuming that $s, s_z \ll s^* \approx s_z^*$ (because of the gravitational friction) and $x \gg x^*$ (both heating and cooling

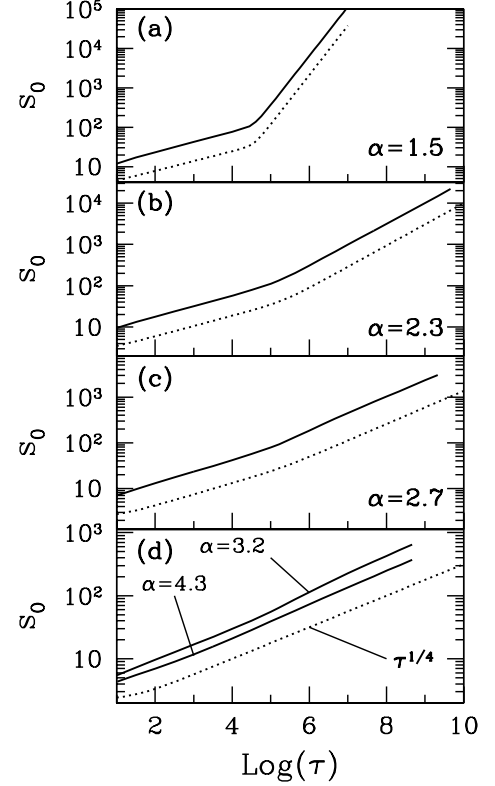


FIG. 4.— Comparison of numerical (*solid curves*) and analytical (*dotted curves*) behaviors of s_0 as a function of dimensionless time τ . We display cases: (a) $\alpha = 1.5$, (b) $\alpha = 2.3$, (c) $\alpha = 2.7$, (d) $\alpha = 3.2$ and $\alpha = 4.3$.

are dominated by planetesimals, not runaway bodies), and neglecting l.h.s. of both equations (similar to the previously discussed situation for $x_c \lesssim x \lesssim x_{shear}$), we obtain the following result:

$$\begin{aligned} s(x, \tau) &\approx x^{-1/6} \left[\frac{M_2(\tau)}{M_1} \right]^{1/2}, \\ s_z(x, \tau) &\approx \frac{1}{\sqrt{x}} \left[\frac{1}{M_1} \int_1^\infty dx^* x^{*2} s^{*2} f(x^*) \right]^{1/2}. \quad (36) \end{aligned}$$

Finally, setting $s^* \approx s_0(\tau)$ as appropriate for $\alpha < 2$ we find that

$$\begin{aligned} s(x, \tau) &\approx x^{-1/6} \left(\frac{\tilde{M}_2}{M_1} x_c \right)^{1/2}, \\ s_z(x, \tau) &\approx s_0 \left(\frac{x_c}{x} \right)^{1/2} \left(\frac{\tilde{M}_2}{M_1} \right)^{1/2}, \quad x \gtrsim x_{shear}. \quad (37) \end{aligned}$$

These expressions demonstrate that transition to the shear-dominated regime is accompanied by a change of the power-law index of eccentricity scaling with mass, while the power-law slope of inclination scaling stays the same. This happens because in the case of inclination evolution heating term is functionally similar to the friction term (exactly like in the dispersion-dominated case), which is not the case for eccentricity evolution, see

(17). As a result, for $x \lesssim x_{shear}$ one finds that $s \gg s_z$ — planetesimal velocity ellipsoid flattens considerably in the vertical direction, which is very unlike the dispersion-dominated case (see Figure 2). This conclusion is very general and should be found whenever runaway bodies interact with *all* planetesimals in the shear-dominated regime.

4.1.3. Comparison with numerical results.

To check the prediction of our asymptotic analysis we have performed numerical calculations of planetesimal velocity evolution for a distribution of planetesimal masses which was artificially evolved in time according to prescriptions outlined in §3. Details of our numerical procedure can be found in Appendix A.

In Figure 3 we show the evolution of planetesimal eccentricity and inclination dispersions for a shallow mass spectrum with $\alpha = 1.5$. For each curve displaying s or s_z run with x at a specific moment of time we also computed power law spectral index $\eta \equiv d \ln s / d \ln x$. We then compare power law indices η and η_z with analytical predictions given by equations (29), (32), & (37). Dotted line in the upper panels of Figure 3 represents analytical predictions for η and η_z at the moment when the snapshot of velocity spectrum displayed by the solid line (corresponding to the highest x_c shown) was taken. One can see that agreement between two approaches is quite good. Power law slopes of both eccentricity η and inclination η_z exhibit a well defined plateau at masses considerably smaller than x_c which is predicted by (29). Above upper mass cutoff η and η_z plunge towards $-1/2$ which is in agreement with (32), although they do not follow this value very closely. The reason is most likely the lack of dynamical range — transitions between different regimes typically occupy substantial intervals in mass. Finally, at x above x_{shear} , where runaway bodies interact with all planetesimals in shear-dominated regime, η goes up to $-1/6$ while η_z stays at a value of $-1/2$, exactly like equation (37) predicts. Glitches in the curves of η and η_z in the vicinity of x_{shear} are the artifacts of interpolation of scattering coefficients between shear- and dispersion-dominated regimes.

In Figure 4a we display the time evolution of s_0 — eccentricity dispersion of smallest planetesimals versus the prediction of our analysis given by equation (29). One can see that the agreement between two approaches is excellent — analytical and numerical results closely follow each other as time increases. Vertical offset between them amounts to a constant factor by which numerically determined $s_0(\tau)$ differs from analytical $s_0(\tau)$. This, of course, is expected because we completely ignored constant coefficients in our asymptotic analysis. Numerical results shown in Figure 4a allow us to fix constant coefficient in (29), and we do this when we calculate x_{shear} in Figure 3 using equation (33). Note that the rapid growth of s_0 with time should certainly increase velocities of planetesimals beyond their escape speeds (if it were not the case initially). Dynamical evolution in this case is discussed in more details in §5.

An apparent break in the behavior of $s_0(\tau)$ at $\tau \sim 10^5$ can be seen in Figure 4a. It occurs because this is the time at which mass scale x_c starts to grow. The prescription for $x_c(\tau)$ which we use (described in Appendix A) is such that x_c is almost constant for $\tau \lesssim 10^5$; as a

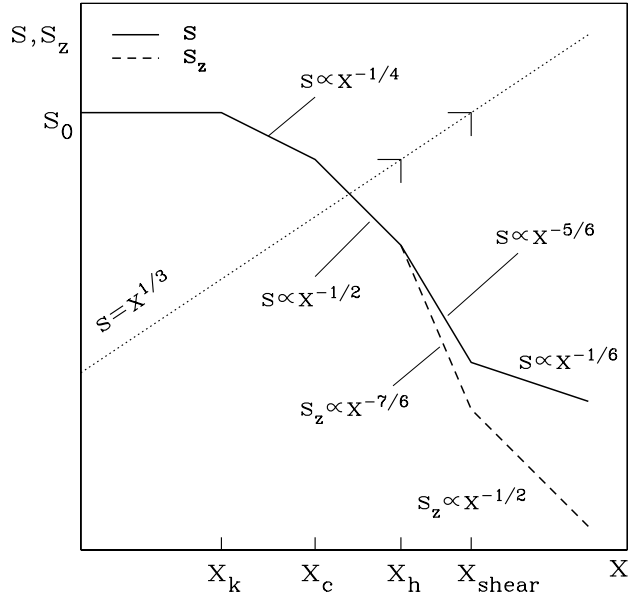


FIG. 5.— Same as Figure 2 but for the case of intermediate mass spectrum. Specific case of $2 < \alpha < 5/2$ is displayed. Notation is explained in the text. Analogous plot for $5/2 \leq \alpha < 3$ would exhibit different behavior of s_z in the high-mass tail and can be easily constructed using the results of §4.2.2.

result, $s_0 \propto \tau^{1/4}$ according to equation (29). At $\tau \gtrsim 10^5$ scale factor starts to increase rapidly and this causes s_0 to grow faster. To conclude, the results of this section show that the overall agreement between numerical calculations and analytical theory of planetesimal velocity evolution is rather good.

4.2. Intermediate mass spectrum.

Self-consistent coagulation calculations (Kenyon & Luu 1998) and N-body simulations of planet formation (Kokubo & Ida 1996, 2000) often yield intermediate mass distributions of planetesimals ($2 < \alpha < 3$). Kokubo & Ida (1996) have found, for example $\alpha \approx 2.5 \pm 0.4$ in their N-body calculation of collisional evolution of several thousand massive ($m = 10^{23}$ g) planetesimals. Such outcome seems to be ubiquitous for planetesimals which agglomerate under the action of strong gravitational focusing (planetesimal velocities are well below the escape velocities from their surfaces) in the dispersion-dominated regime, which makes the case of intermediate mass spectra very important.

4.2.1. Velocities of planetesimals.

As in §4.1 we start our consideration of mass spectra with $2 < \alpha < 3$ by concentrating on planetesimals with masses $\lesssim x_c(\tau)$, assuming that all these bodies interact in the dispersion-dominated regime (see §4). Then equations (26) and (27) continue to hold.

It is natural to start by assuming again that s is independent of x . Performing analysis similar to that of §4.1.2 we find that stirring is still dominated by large planetesimals ($\sim x_c$), but the biggest contribution to the gravitational friction is produced by smallest planetesimals (with $m \sim m_0$, or $x \sim 1$ in our dimensionless

notation):

$$\frac{\partial s^2}{\partial \tau} \approx A_1 \frac{x^{3-\alpha}}{2s^2} - 2A_2 \frac{x}{4s^2} M_1 + (A_1 - A_2) \frac{M_2(\tau)}{2s^2}. \quad (38)$$

Clearly, the first term on the r.h.s. which is responsible for the stirring by small planetesimals is negligible compared to the last one, representing stirring by planetesimals bigger than x [see (24)]. Also, by definition, M_1 is just a dimensionless total surface density of planetesimal disk, and thus has to be constant in time. Then our assumption of s independent of x is self-consistent and s is given by the first equality in (29) only if friction by small planetesimals [second term in (38)] is small compared to stirring by big ones (third term), which is true provided that

$$x \lesssim x_k(\tau) \equiv \frac{M_2(\tau)}{M_1} = x_c \frac{\tilde{M}_2}{M_1} x_c^{2-\alpha} \ll x_c. \quad (39)$$

The last equality follows from the fact that $M_2 = \tilde{M}_2 x_c^{3-\alpha}$ when $2 < \alpha < 3$. Thus, for small planetesimals ($x \lesssim x_k$) friction by even smaller ones is again unimportant; their velocities are excited by big planetesimals ($x \sim x_c$), and as a result [cf. (29)]

$$s(x, \tau) \approx s_0(\tau) = \left[\tilde{M}_2 \int_1^\tau [x_c(\tau')]^{3-\alpha} d\tau' \right]^{1/4} \\ = \text{const}(x), \quad 2 < \alpha < 3, \quad x \lesssim x_k. \quad (40)$$

However, for $x \gtrsim x_k$, gravitational friction by small planetesimals is no longer negligible compared to the velocity excitation by big ones. One would then expect friction to lower the velocities of big bodies below those of small planetesimals (because of the tendency to energy equipartition associated with friction term). Starting with (27) and using (40) we obtain the following equation for $x \gtrsim x_k$:

$$\frac{\partial s^2}{\partial \tau} = \frac{A_1}{s_0^2} \int_1^{\sim x_k} dx^* (x^*)^2 f(x^*) + A_1 \int_{\sim x_k}^x dx^* \frac{(x^*)^2 f(x^*)}{s^{*2}} \\ - 2A_2 \frac{s^2 x}{s_0^4} \int_1^{\sim x_k} dx^* x^* f(x^*) - 2A_2 s^2 x \int_{\sim x_k}^x dx^* \frac{x^* f(x^*)}{s^{*4}} \\ + \frac{A_1 - 2A_2}{s^2} \int_{\sim x}^\infty dx^* (x^*)^2 f(x^*). \quad (41)$$

In this equation different terms represent stirring or friction by different parts of planetesimal mass spectrum, below and above x_k . We now take an educated guess that the solution for s can be obtained by equating third and fifth terms in the r.h.s. of (41). Physically this means that velocity spectrum results from the balance of velocity stirring by biggest planetesimals (masses $\sim x_c \gg x$, similar to the case of shallow mass spectrum) and friction which is mainly contributed by smallest planetesimals. One then finds that [see (39)]

$$s(x, \tau) \approx s_0(\tau) \left[\frac{M_2(\tau)}{M_1} \right]^{1/4} x^{-1/4} \\ \approx s_0(\tau) \left[\frac{x_k(\tau)}{x} \right]^{1/4}, \quad x_k \lesssim x \lesssim x_c. \quad (42)$$

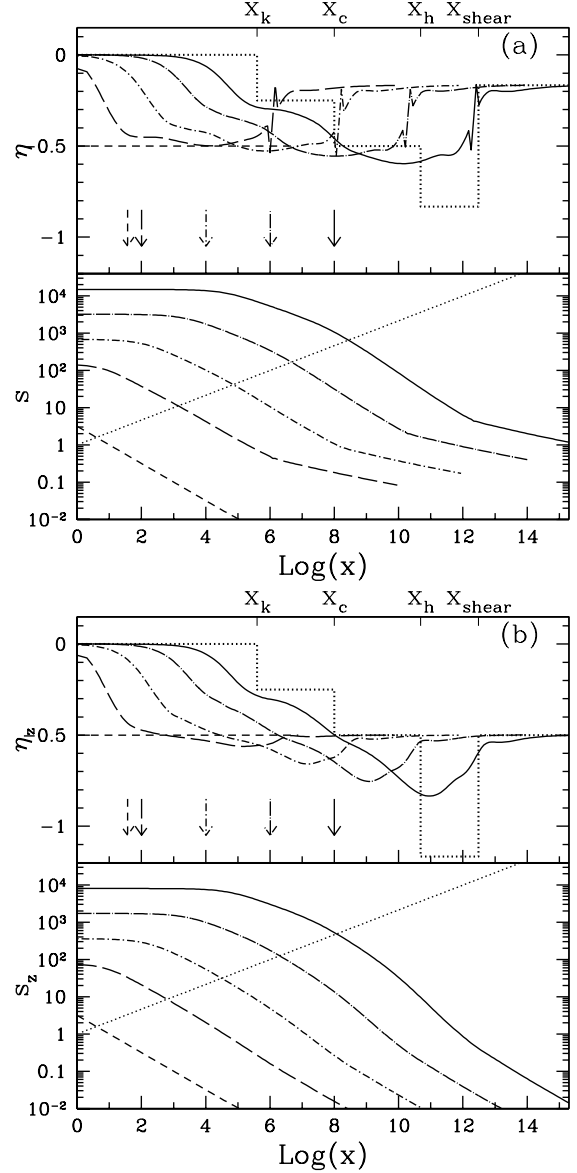


FIG. 6.— The same as Figure 3 but for the case of intermediate mass spectrum with $\alpha = 2.3$ (cf. Fig. 5).

Substituting this solution into (41) we easily verify that our neglect of all other terms in the r.h.s. of (41) is indeed justifiable. The l.h.s. of (41) can be neglected for $x_k \lesssim x \lesssim x_c$ on the basis of arguments identical to those advanced in §4.1.2. Thus, s given by (42) is indeed a legitimate solution in this mass range.

Equations (40) & (42) highlight an interesting feature of the case $2 < \alpha < 3$: although the mass spectrum has a power law form with a continuous slope all the way up to x_c , velocity spectrum exhibits a knee at some intermediate mass x_k (see Figure 5). The resemblance of the velocity spectrum for $x \lesssim x_k$ to the spectrum for $\alpha < 2$ is due to the fact that in both cases stirring is done by biggest planetesimals and friction has a small effect. However, for $x \gtrsim x_k$ effect of friction becomes important, and now it is dominated by the part of mass spectrum (smallest planetesimals) different from that responsible for stirring (biggest planetesimals). This causes velocity

spectrum to change its slope from 0 to $-1/4$ in this mass range (see Figure 5).

4.2.2. Velocities of runaway bodies.

Similar to the case of shallow mass spectrum, some (lightest) runaway bodies interact with the bulk of planetesimals in the dispersion-dominated regime. In this case all the considerations of §4.1.2 hold, i.e. evolution equation (30) stays unchanged and after the same line of arguments we arrive at the expression (31) for the planetesimal velocity dispersion. Integrals entering (31) must be reevaluated anew using equations (40) & (42) appropriate for $2 < \alpha < 3$. Performing this procedure and substituting resulting expressions into (31) we find that

$$\begin{aligned} s(x, \tau) &\approx \frac{s_0}{\sqrt{x}} \left[\frac{M_{5/2}(\tau)}{M_1 x_k^{1/2}(\tau)} \right]^{1/2} \\ &= s_0 \left(\frac{x_c}{x} \right)^{1/2} \left(\frac{\tilde{M}_{5/2}}{\tilde{M}_2} \sqrt{\frac{x_k}{x_c}} \right)^{1/2}, \quad x_c \lesssim x \lesssim x_h. \end{aligned} \quad (43)$$

This velocity distribution is valid only for runaway bodies lighter than

$$x_h \equiv [s(x_c)]^3 \approx s_0^3 \left(\frac{x_k}{x_c} \right)^{3/4}, \quad (44)$$

because only such bodies interact with *all* small mass planetesimals ($x \lesssim x_c$) in the dispersion-dominated regime. In agreement with what we found earlier in §4.1.2, velocity dispersion decreases with mass as $x^{-1/2}$. At $x \sim x_c$ this expression matches the low mass result (42).

Runaway bodies heavier than x_h but still lighter than $x_{shear} \equiv s_0^3$ are in a mixed state: they interact with the most massive planetesimals in the shear-dominated regime, and with lighter ones in the dispersion-dominated regime. This, of course, is a direct consequence of the fact that the velocity spectrum of planetesimals has a knee at x_k , see §4.2.1. Introducing

$$x_s(x) \equiv x_k \left(\frac{s_0}{x^{1/3}} \right)^4. \quad (45)$$

we find that runaway bodies with masses x between x_h and x_{shear} interact with planetesimals less massive than $x_s(x)$ in the dispersion-dominated regime, and with planetesimals heavier than $x_s(x)$ in the shear-dominated regime. Self-consistent analysis of planetesimal velocity spectrum for $x_h \lesssim x \lesssim x_{shear}$ is described in detail in Appendix B, and only final results are shown here. It turns out that eccentricity scales as

$$s(x, \tau) \approx \frac{s_0}{x^{5/6}} \left[s_0^2 \frac{M_2(\tau)}{M_1} \right]^{1/2} = s_0 \frac{s_0 x_k^{1/2}}{x^{5/6}}, \quad x_h \lesssim x \lesssim x_{shear}, \quad (46)$$

while inclination behaves in a different manner:

$$\begin{aligned} s_z(x, \tau) &\approx \frac{s_0}{x^{7/6}} \left[s_0^4 x_k^{1/2} \frac{M_{3/2}(\tau)}{M_1} \right]^{1/2} \\ &= \frac{s_0}{x^{7/6}} \left[s_0^4 x_k \left(\frac{x_k}{x_c} \right)^{1/2} \frac{\tilde{M}_{3/2}}{\tilde{M}_2} \right]^{1/2}, \quad \alpha < 5/2, \end{aligned} \quad (47)$$

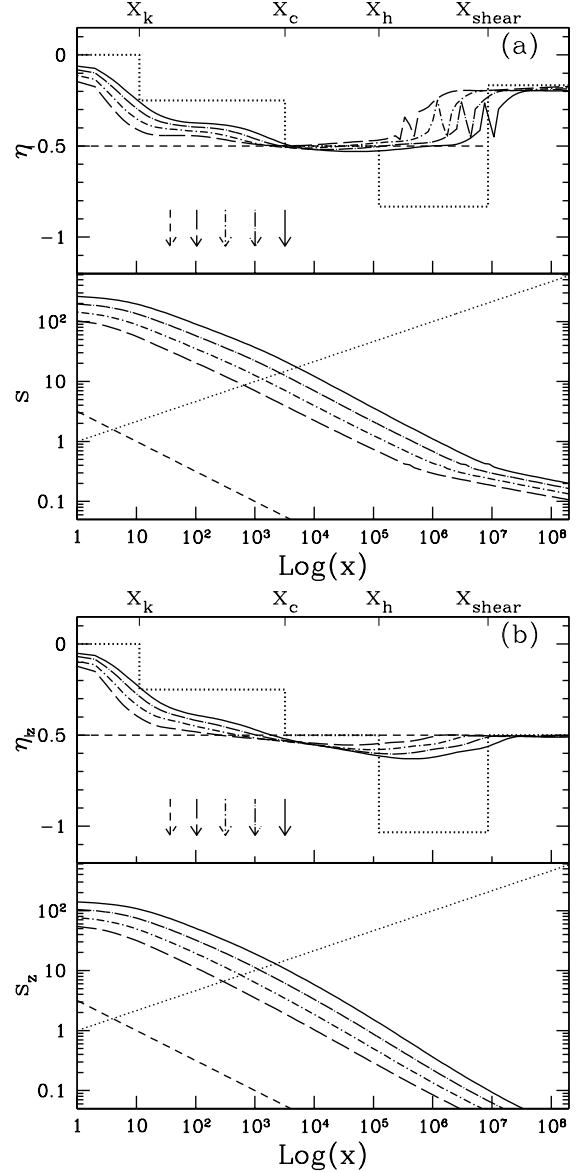


FIG. 7.— The same as Figure 3 but for the case of intermediate mass spectrum with $\alpha = 2.7$ (cf. Fig. 5).

$$\begin{aligned} s_z(x, \tau) &\approx s_0 \left[\frac{(x_s(x))^{7/2-\alpha}}{x_k^{1/2} x M_1} \right]^{1/2} \\ &\propto x^{(4\alpha-17)/6}, \quad \alpha > 5/2, \end{aligned} \quad (48)$$

In the case of $\alpha = 5/2$ a more general expression for s_z following directly from (B4) should be used.

Finally, bodies heavier than x_{shear} interact with *all* planetesimals in the shear-dominated regime. Expressions (36) adequately describe velocity behavior in this case. Manipulating them with the aid of equations (40) and (42) we find that

$$s(x, \tau) \approx \frac{x_k^{1/2}}{x^{1/6}}, \quad x \gtrsim x_{shear}. \quad (49)$$

while

$$s_z(x, \tau) \approx s_0 \left(\frac{x_k}{x} \right)^{1/2} \left[\left(\frac{x_k}{x_c} \right)^{1/2} \frac{\tilde{M}_{3/2}}{\tilde{M}_2} \right]^{1/2},$$

$$\alpha < 5/2, \quad (50)$$

$$s_z(x, \tau) \approx s_0 \left(\frac{x_k}{x} \right)^{1/2} \left(\frac{x_k}{x_c} \right)^{(3-\alpha)/2}, \quad \alpha > 5/2. \quad (51)$$

Scalings of velocity dispersions with mass x in (49)-(51) are the same as in the case of shallow mass spectrum, but the time dependences are different. Velocity behavior in the case of intermediate mass spectrum is displayed in Figure 5.

4.2.3. Comparison with numerical results.

We calculated numerically the evolution of s and s_z for two intermediate mass spectra: $\alpha = 2.3$ and $\alpha = 2.7$. In Figure 4b,c we compare numerically calculated $s_0(\tau)$ — eccentricity dispersion of smallest planetesimals — with predictions of our asymptotic theory. As in the case of shallow mass spectrum discussed in §4.1.3, agreement between the two approaches is very nice. This allows us to fix coefficient in (40), absence of which in our asymptotic analysis causes a constant offset between numerical and analytical curves in Figure 4b,c. Results for the velocity dependencies on mass at different moments of time and their comparison with analytical theory of intermediate mass spectra outlined above are shown in Figures 6 and 7.

In the case $\alpha = 2.3$ one can clearly see the appearance of all features we described in §4.2.1 and §4.2.2. Indeed, in Figure 6 one can observe both the zero-slope part of the spectrum at $x \lesssim x_k$ and the trend of reaching the slope $-1/4$ for $x_k \lesssim x \lesssim x_c$; the last feature is not fully developed when we stop our calculation but it is almost certain that η and η_z would reach slope $-1/4$ given enough time and mass range. Calculation has to be stopped when x reaches $\sim 10^8$ because later on biggest planetesimals start interacting with bodies of similar size in the shear-dominated regime. Such a possibility was not explicitly considered in the present study (but it can be easily dealt with using analytical apparatus developed in this work).

Results for biggest runaway bodies ($x \gtrsim x_{shear}$) are in nice concordance with analytical predictions given by equations (51). In the range $x_c \lesssim x \lesssim x_{shear}$ velocities of the runaway bodies clearly have not yet converged to a steady state but are evolving in the right direction. The range of masses where velocity spectrum should exhibit a slope $-1/2$ [$x_c \lesssim x \lesssim x_h$, see (43)] is so narrow⁶ for the last (solid) curve (because planetesimals with mass $\sim x_c$ are already very close to shear-dominated regime) that we do not see this regime realized. At the same time, it is conceivable that runaway bodies which interact with planetesimals in the mixed regime ($x_h \lesssim x \lesssim x_{shear}$, see Appendix B) will finally reach their asymptotic velocity state with $\eta = -5/6$ and $\eta_z = -7/6$ [see equation (48)], although it will take very long time for them to get there.

Comparison for the case $\alpha = 2.7$ (Figure 7) is very similar. All major features corresponding to the intermediate mass spectrum can be traced in this case as well. Unfortunately, the comparison with analytical results is complicated by the fact that in this case we have to stop

⁶ Position of x_h in Figure 6 is determined by equation (44) which assumes that between x_k and x_c velocity behaves $\propto x^{-1/4}$. In reality, as we discussed above, velocity slope in that mass region is somewhat steeper causing (44) to overestimate x_h .

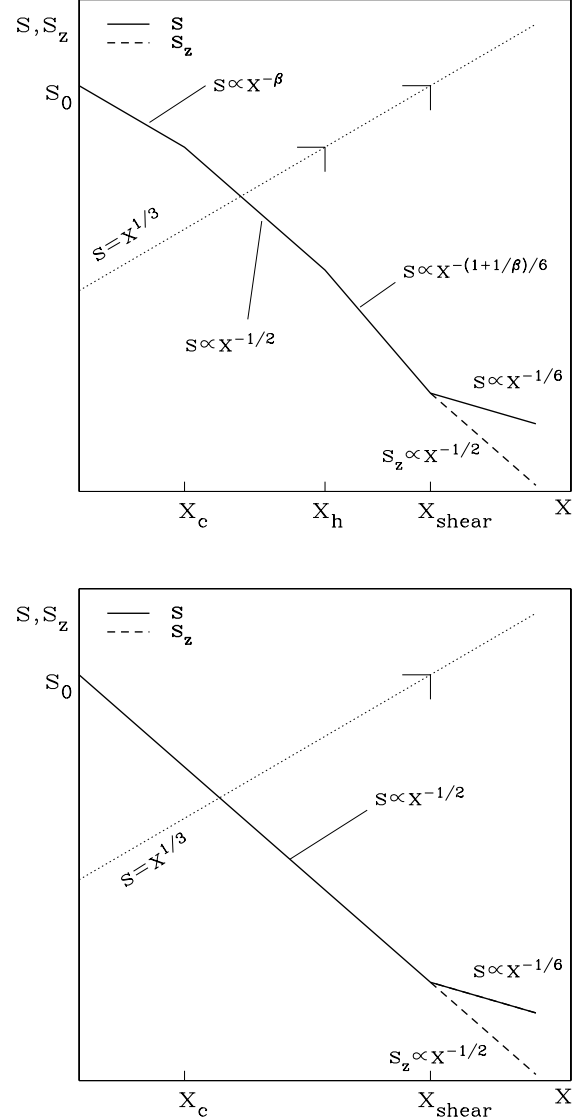


FIG. 8.— (a) Same as Figure 2 but for the Case 1 of steep mass spectrum ($3 < \alpha < 4$). Note that $1/4 < \beta < 1/2$ [see equation (55)]. (b) Same as Figure 2 but for steep mass spectrum with $\alpha > 4$.

numerical calculation even earlier than in $\alpha = 2.3$ case to avoid bringing most massive planetesimals into the shear-dominated regime (for this reason mass scale in Figure 7 does not go as far as in Figure 6). As a result, even a velocity plateau at small masses does not have time to fully develop, not speaking of runaway bodies in “mixed” interaction state. Despite this, the overall agreement between the numerical results and asymptotic theory of velocity evolution of intermediate mass distributions is rather good, especially if we make allowance for the short duration of our calculation and small mass range of planetesimals.

4.3. Steep mass spectrum.

Planetesimal spectra decreasing with mass steeper than m^{-3} are usually not found in calculations of planetesimal agglomeration. Still, this case is quite interest-

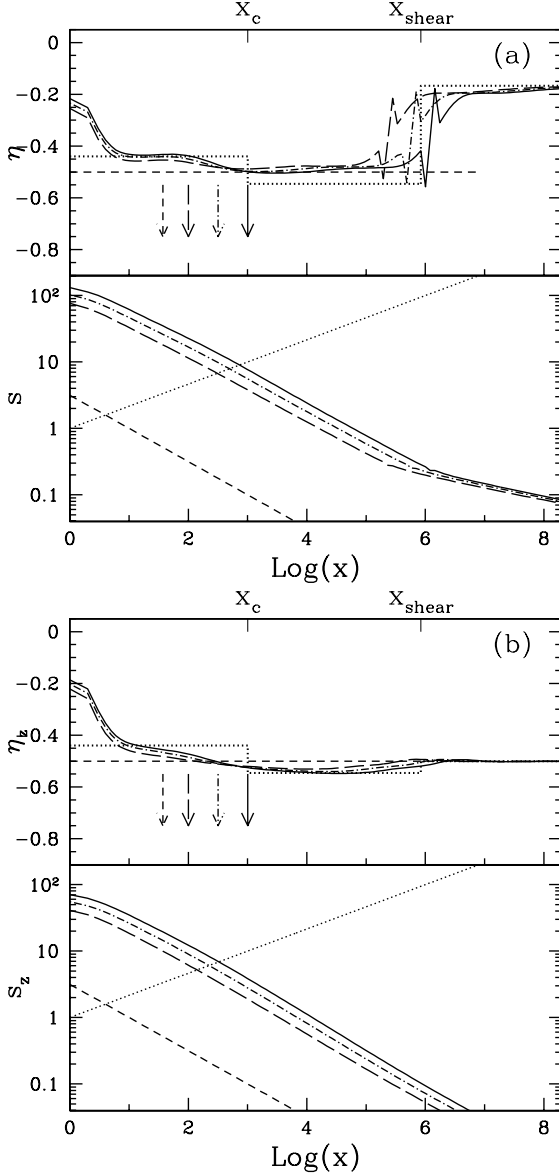


FIG. 9.— The same as Figure 3 but for the case of steep mass spectrum with $\alpha = 3.2$ (cf. Fig. 8a).

ing and we briefly discuss it here.

As demonstrated in §4.1 & §4.2 stirring of planetesimals is determined solely by biggest bodies with masses $\sim x_c$ when $\alpha < 3$. This is no longer true when the mass spectrum becomes steeper than x^{-3} . Indeed, let us consider the evolution of s_0 — velocity dispersion of *smallest* planetesimals having dimensionless mass $x = 1$. Using equation (26) we find that

$$\frac{\partial s_0^2}{\partial \tau} \approx \frac{1}{s_0^2} \int_1^\infty dx^* f(x^*) \frac{x^*(x+x^*)}{1+s^{*2}/s_0^2} \times \left[\frac{x^*}{x+x^*} A_1 - 2 \frac{1}{1+s^{*2}/s_0^2} A_2 \right] \quad (52)$$

Assuming that $s^*/s_0 \rightarrow 0$ when $x^*/x \rightarrow \infty$ as a result of gravitational friction we find that integral in (52) is dominated by its lower integration limit for $\alpha > 3$. This means that the velocity of smallest planetesimals is

now mediated by smallest planetesimals themselves, unlike the case of $\alpha < 3$. We also find that the temporal behavior of s_0 is given simply by

$$s_0(\tau) \approx \tau^{1/4}, \quad \alpha > 3. \quad (53)$$

We now turn our attention to studying planetesimal velocities in the mass range $1 \lesssim x \lesssim x_c$. We make an a priori assumption that planetesimal velocity spectrum has a form of a simple power law (with constant power law index)

$$s(x, \tau) \approx s_0(\tau) x^{-\beta}, \quad x \lesssim x_c, \quad (54)$$

and verify later if it is correct. In Appendix C we show that whenever $3 < \alpha < 4$, both heating and friction of planetesimals of a particular mass x are determined by bodies of similar mass, $x^* \sim x$. This is somewhat unusual in view of our previous results when only the extrema of power-law mass spectrum were important (see §4.1 and §4.2. In this case power law index β can only be found by numerically solving equation (C2); there is no simple expression for β but its value has to satisfy condition

$$\frac{\alpha - 2}{4} < \beta < \frac{1}{2}. \quad (55)$$

For even steeper mass distributions, $\alpha > 4$, we demonstrate in Appendix C that smallest planetesimals dominate both stirring and friction not only of themselves, but also of bigger bodies. This occurs because mass spectrum is very steep and high mass planetesimals contain too little mass to be of any dynamical importance. This is very similar to the velocity evolution of the runaway tail in the dispersion-dominated regime described in §4.1.2, and, not surprisingly, we find that $\beta = 1/2$ when $\alpha > 4$. Thus, a solution leading to a complete energy equipartition between planetesimals ($s \propto x^{-1/2}$) is only possible for very steep mass spectra. Velocity behavior of runaway bodies in the case of steep mass spectrum is described in detail in Appendix C. Theoretical spectra of planetesimal velocities are schematically illustrated in Figures 8a (for $3 < \alpha < 4$) and 8b (for $\alpha > 4$).

We verify the accuracy of these predictions by numerically calculating the velocity evolution of planetesimal disks with $\alpha = 3.2$ and $\alpha = 4.3$. In the first case, shown in Figure 9, the slope β of planetesimal velocity spectrum for $x \lesssim x_c$ is evidently shallower than $-1/2$ but steeper than $-(\alpha - 2)/4 = -0.3$, in agreement with constraint (55). Analytical prediction for the behavior of $\eta(x)$ in top panels of Figure 9 is computed using the numerically determined value of β and equations (C4), (C5), and (C6). It agrees with numerical result (solid curves corresponding to the largest x_c displayed) rather well, especially for $x \gtrsim x_{shear}$.

In the case $\alpha = 4.3$ (Figure 10) the slope of planetesimal velocity scaling with mass is essentially indistinguishable from $-1/2$ for $x \lesssim x_c$, in accordance with our asymptotic prediction. Velocity evolution of runaway tail also agrees with the discussion in Appendix C.2 quite well. In both $\alpha = 3.2$ and $\alpha = 4.3$ cases the final velocity curves displayed are at the limit where we can still apply our theory: $s(x_c) \sim x_c^{1/3}$; this washes out some details of velocity spectra of runaway tails predicted in Appendix C.2. Differences of η and η_z from their predicted values at smallest planetesimal masses are caused by boundary

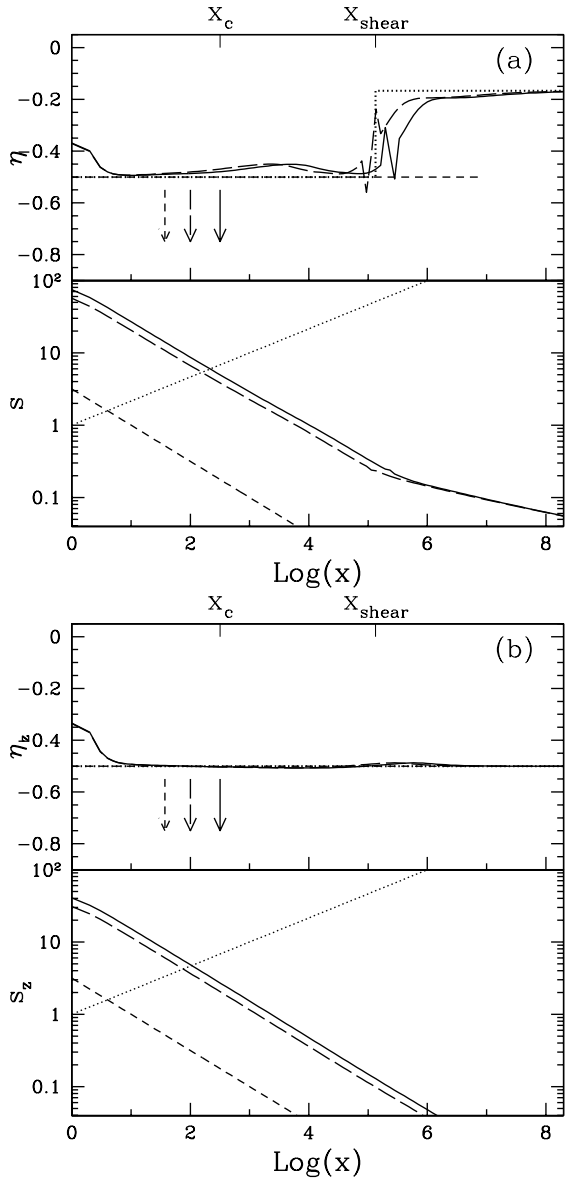


FIG. 10.— The same as Figure 3 but for the case of steep mass spectrum with $\alpha = 4.3$ (cf. Fig. 8b).

effects. Note that the eccentricity dispersion s is virtually independent of time above x_{shear} for both $\alpha = 3.2$ and 4.3 (while inclination dispersion s_z slowly grows as τ increases), which is in complete agreement with equation (C6). Finally, numerically computed $s_0(\tau)$ follows reasonably well analytical result represented by formula (53), which is demonstrated in Figure 4d.

5. VELOCITY SCALING IN THE PRESENCE OF DISSIPATIVE EFFECTS.

Until now we have been assuming that gravity is the only force acting on planetesimals. In reality there should be other factors such as gas drag and inelastic collisions between planetesimals which might influence their eccentricities and inclinations. Here we briefly comment on the possible changes these effects can give rise to.

In the presence of gas drag eccentricity and inclination of a particular planetesimal with mass m and physical

size r_p tend to decrease with time. Adachi et al. (1976) investigated the damping of planetesimal eccentricities and inclinations assuming gas drag force proportional to the square of planetesimal velocity relative to the gas flow. They came out with orbit-averaged prescription for the evolution of random velocity of planetesimals which can be written at the level of accuracy we are pursuing in this study (dropping all possible constant factors and assuming that eccentricity is of the same order as inclination) as

$$\frac{\partial e^2}{\partial t} \approx -e^2(e + \eta) \frac{\rho_g \Omega a}{\rho_p r_p}, \quad (56)$$

where ρ_g is the mass density of nebular gas, ρ_p is the physical density of planetesimal, and $\eta \equiv (c_s/\Omega a)^2 \ll 1$, with c_s being the sound speed of nebular gas. In our notation (see §2) this equation translates into

$$\begin{aligned} \frac{\partial s^2}{\partial \tau} &\approx -\zeta s^2 x^{-1/3} \left[s + \eta \left(\frac{M_c}{m_0} \right)^{1/3} \right], \\ \zeta &\equiv \frac{\Sigma_g \Omega a}{\Sigma_p c_s} \left[\frac{m_0 M_c}{(\rho_p a^3)^2} \right]^{1/3} \\ &\approx 10^{-6} a_{AU}^{-5/2} \left(\frac{\Sigma_g/\Sigma_p}{100} \right) \left(\frac{1 \text{ km s}^{-1}}{c_s} \right) \left(\frac{m_0}{10^{18} \text{ g}} \right)^{1/3} \end{aligned} \quad (57)$$

where Σ_g is the surface mass density of the gas disk, and numerical estimate is made for $\rho_p = 3 \text{ g cm}^{-3}$ and $M_c = M_\odot$. For protoplanetary nebula consisting of solar metallicity gas one would expect $\Sigma_g/\Sigma_p \approx 50 - 100$, but during the late stages of nebula evolution this ratio should be greatly reduced by gas removal⁷.

We use the results of §4 to discuss the effect of the gas drag on the planetesimal random velocities for mass distributions with $\alpha < 3$. We know from §4.1 and §4.2 that stirring in this case is dominated by biggest planetesimals and stirring rate is $\approx M_2(\tau)/s^2$ [see equations (28), (38), and (41)]. Comparing this heating rate with damping due to gas drag (57) we immediately see that gas drag can become important for small planetesimals if planetesimal velocities are large ($s \gg 1$). In this case dynamical excitation by biggest planetesimals is balanced by gas drag. Very interestingly, it turns out that such a balance leads to $s \propto x^{1/12}$ or $x^{1/15}$ (depending on whether s is bigger or smaller than $\eta(M_c/m_0)^{1/3}$), i.e. smaller planetesimals have smaller random velocities. Such a behavior has been previously seen in coagulation simulations including effects of gas drag on small planetesimals (e.g. Wetherill & Stewart 1993). The time dependence of velocities of small planetesimals affected by the gas drag should also be different from that given by (29) or (40). In Figure 11 we schematically display the scaling of s as a function of x in the presence of gas drag for $2 < \alpha < 3$ and different values of ζ .

Inelastic collisions between planetesimals become important for their dynamical evolution roughly when relative velocity at infinity with which two planetesimals approach each other becomes comparable to the escape speed from the biggest of them; in this case gravitational

⁷ Note that for planet formation in some exotic environments such as early Universe prior to metal enrichment or metal-poor globular clusters this ratio can be much larger than 100.

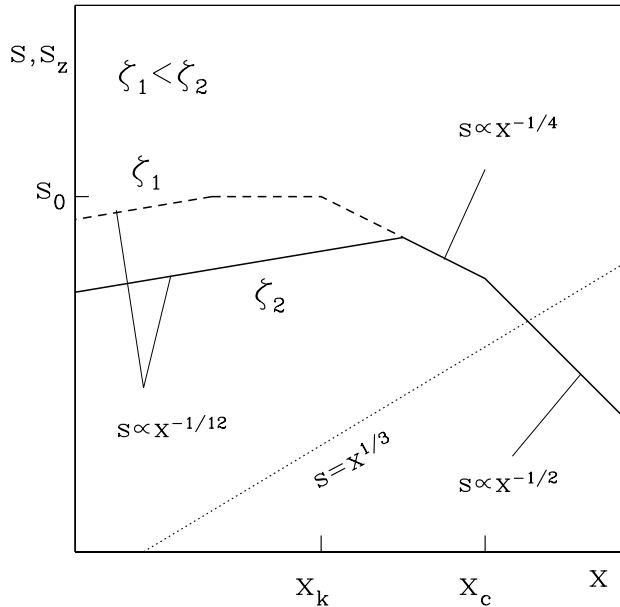


FIG. 11.— Schematic representation of the effect of gas drag on planetesimal velocity spectrum in the case $2 < \alpha < 3$ (cf. Figure 5). Velocity dependence on planetesimal mass is displayed for two values of gas drag parameter ζ defined by equation (57): ζ_1 (dashed curve) and ζ_2 (solid curve), with $\zeta_1 < \zeta_2$. Velocity spectra overlap at high masses for which gas drag is no longer important. Inelastic collisions between planetesimals would affect their velocity spectrum in a similar manner.

focusing is inefficient. The escape speed $v_{esc} \approx 1 \text{ m s}^{-1} r_p / (1 \text{ km})$ (for physical density $\rho = 3 \text{ g cm}^{-3}$) is much larger than the Hill velocity for the same mass $\Omega R_H \approx 5 \text{ cm s}^{-1} a_{AU}^{-1/2} r_p / (1 \text{ km})$ (for $M_c = M_\odot$), which justifies initially our previous neglect of inelastic collisions (especially far from the Sun where ΩR_H is small). Later on, however, continuing dynamical heating in the disk would certainly bring velocities of small planetesimals above their escape speeds. When this happens, collisions with bodies of similar size lead to strong velocity dissipation. This damping should produce similar effect on planetesimal random velocities as gas drag does. Indeed, kinetic energy losses in physical collisions between high velocity planetesimals are roughly proportional to their initial kinetic energies, which is similar to the behavior of the gas drag losses.

At the same time, velocities of light bodies should still be smaller than the escape velocity from the biggest planetesimals, since otherwise these planetesimals would not be able to dynamically heat the disk and it would “cool” below their escape velocity. Thus, planetesimal velocities cannot exceed the escape speed from the surfaces of bodies doing most of the stirring, result dating back to a classical study by Safronov (1972). This implies that gravitational stirring must still be done by the highest mass planetesimals (if $\alpha < 3$) in accordance with what we assumed in the case of gas drag. As a result, one would again expect s to exhibit a power law dependence on mass with positive (but small) slope. Exact value of the power law index of this dependence is determined by the scaling of energy losses with the mass of planetesimals

involved in collision⁸. Effect of the collisions should be most pronounced for small planetesimals for which relative encounter velocities can be much higher than their v_{esc} . Threshold mass at which highly inelastic collisions become important must constantly increase in time as planetesimal disk is heated up by massive planetesimals. One should also remember that planetesimal fragmentation in high velocity encounters may become important in this regime which would significantly complicate simple picture we described here.

In summary, dissipative effects are unlikely to affect the dynamics of massive planetesimals. However, they become important for small mass planetesimals and lead to positive correlation between random velocities of planetesimals and their masses (unlike the case of pure gravity studied in §4), which has been previously observed in self-consistent coagulation simulations (Wetherill & Stewart 1993). It is thus fairly easy to modify our simple picture developed in §4 to incorporate the effects of gas drag and inelastic collisions.

6. DISCUSSION.

Although our study has concentrated on a particular case of power-law size distributions (most of the mass is locked up in the power-law part of the planetesimal mass spectrum) its results have a wider range of applicability. The reason for this is that the velocity scalings derived in §4 depend only on what part of planetesimal spectrum dominates stirring and friction and not on the exact shape of mass distribution. For example, suppose that $f(x, \tau)$ does not have a self-similar power law form of the kind studied in §4.2 (intermediate mass spectrum) but its first moment M_1 is still dominated by the smallest masses (most of the mass is locked up in smallest planetesimals, which dominate friction), while the second moment M_2 is mainly determined by highest masses (heating is determined by biggest planetesimals $\sim x_c$). Then it is easy to see from our discussion in §4.2.1 that the velocity distribution has a form of a broken power-law in mass, changing its slope from 0 at small masses to $-1/4$ at high masses [see (40) and (42)]. If, on the contrary, most of the mass is not in smallest bodies but in largest ones (M_1 and M_2 converge near the cutoff of planetesimal spectrum, $\sim x_c$), then both friction and stirring are dominated by biggest planetesimals and velocity spectrum must have zero slope for the entire range of planetesimal masses, in accord with our consideration of shallow mass distributions (§4.1.1). Whenever both stirring and cooling of planetesimals of mass m are dominated by planetesimals of similar mass, we go back to the Case 1 of §4.3. Finally, in all cases when stirring and friction are produced by planetesimals much smaller than those under consideration, velocity profile scales like $m^{-1/2}$ (energy equipartition, see Case 2 in §4.3). Similar rules can be derived on the basis of the results of §4 for more complicated mass spectra, and this makes our approach very versatile.

One of the interesting features found in our study of purely gravitational scattering (see §4) is the develop-

⁸ Note that in the crude picture of collision energy losses mentioned above $d\sigma_e^2/dt$ is independent of planetesimal mass. Then the power law index of velocity spectrum of small planetesimals is exactly zero. More accurate treatment of planetesimal collisions might result in some mass dependence of random velocities.

ment of a plateau at the low mass end of planetesimals velocity distribution for shallow and intermediate mass spectra ($\alpha < 3$). These mass spectra are among the most often realized in the coagulation simulations which makes this prediction quite important for interpretation of numerical results. One should be cautious enough not to confuse these plateaus with the manifestations of dissipative processes such as gas drag or inelastic collisions which tend to endow velocity distribution with only very weak (positive) dependence on mass, see §5.

Another observation which can be made based on our results is that the bulk of planetesimals (power law part where most of the mass is locked up) rarely reaches a complete equipartition in energy. Equipartition is realized when $\sigma_{e,i} \propto m^{-1/2}$, or in our notation $s, s_z \propto x^{-1/2}$. Our calculations (§4.3) show that when $x \lesssim x_c$ such a velocity spectrum is only possible for very steep mass distributions, $\alpha > 4$, when both dispersion-dominated stirring and friction are due to the smallest planetesimals with masses $m \sim m_0$ ($x \sim 1$). Mass distributions that steep are not often encountered in self-consistent coagulation or N-body simulations (Wetherill & Stewart 1993; Kenyon 2002; Kokubo & Ida 1996, 2000) and yet the equipartition argument is very often used to draw important conclusions about the bulk of planetesimal population (see below).

At the same time, random energy equipartition is ubiquitous for runaway bodies in the high mass tail ($x \gtrsim x_c$) if they still interact with the rest of planetesimals in the dispersion-dominated regime. Since, by our assumption, runaway tail contains very little mass, this equipartition is very similar to the case of $\alpha > 4$, because in both situations stirring as well as friction are driven by planetesimals much lighter than the bodies under consideration. It is also worth mentioning that this conclusion changes when runaway bodies start interacting with small planetesimals in the shear-dominated regime (see e.g. §4.1.2).

Although we did not follow the evolution of the planetesimal mass spectrum self-consistently we can already constrain some of the theories explaining mass distributions in coagulation cascades. For example, N-body simulations of gravitational agglomeration of $10^3 - 10^4$ massive planetesimals by Kokubo & Ida (1996, 2000) produce roughly power law mass spectrum with an index of ≈ -2.5 within some range of masses. To explain this result Makino et al. (1998) explored planetesimal growth in the dispersion-dominated regime with strong gravitational focusing. They postulated epicyclic energy to be in equipartition and found that planetesimal mass distribution has a power-law form with a slope of $-8/3 \approx -2.7$. However, using the results of §4.2.1 one can immediately pinpoint the contradiction with the basic assumptions which lead to this conclusion. Indeed, slope of $-8/3$ corresponds to the intermediate mass spectrum (see §4.2) which can never reach energy equipartition. Moreover, this mass spectrum cannot even have a power-law velocity distribution with a continuous slope necessary for a theory of Makino et al. (1998) to work. As a result, the explanation provided by these authors for the mass spectrum found in N-body simulations cannot be self-consistent. More work in this direction has to be done.

Although theory developed in §4 is in good agreement with our numerical calculations, one should bear in mind

that our analytical results are asymptotic by construction, i.e. they are most accurate when planetesimal disk has evolved for a long time and when planetesimal size distribution spans a wide range in mass (this can be easily seen by comparing Figures 6 and 7). Real protoplanetary disks during their evolution might not enjoy the luxury of having such conditions been fully realized; this can complicate quantitative applications of our results to real systems. We believe however that this does not devalue our analytical results because they provide basic understanding of processes involved in planet formation, allow one to clarify important trends seen in simulations, and enable quick and efficient classification of possible evolutionary outcomes for a wide range of parameters of protoplanetary disks.

Several previous studies have concentrated on exploring velocity equilibria in systems with nonevolving mass spectra in which inelastic collisions between planetesimals acted as damping mechanism necessary to balance gravitational stirring (Kaula 1979; Hornung, Pellat, & Barge 1985; Stewart & Wetherill 1988). We have outlined a qualitative picture of the effects of dissipative processes in §5 and it agrees rather well with these previous investigations. N-body calculations and “particle in a box” coagulation simulations represent another class of studies in which velocity distributions have been routinely computed. As we already commented in §1 these calculations usually absorb a lot of diverse physical phenomena which makes them not easy targets for comparisons. Still, there are several generic features almost all simulations agree upon such as (1) roughly power-law mass spectra typically with slopes $\alpha < 3$ within some mass range, (2) velocity dispersion is constant or slowly increases with mass for small planetesimals, and (3) it decreases with mass for large bodies. This general picture is in good agreement with our analytical predictions.

7. CONCLUSIONS.

We have carried out an exhaustive census of the dynamical properties of planetesimal disks characterized by a variety of mass distributions. Here we briefly summarize our results for the case velocity evolution driven by gravitational scattering of planetesimals.

Whenever planetesimal mass distribution in a disk has a power law slope shallower than -2 , we find that planetesimal velocity is constant up to the upper mass cutoff. For slopes between -2 and -3 velocity dispersions are constant at small masses but switch to $m^{-1/4}$ dependence above some intermediate mass. As a result, mass spectrum exhibits a pronounced “knee” at this mass. Distributions with slopes between -3 and -4 have purely power-law velocity spectra with slope $-\beta$ satisfying $1/4 < \beta < 1/2$, which can be determined numerically using equation (C2). Finally, planetesimals in disks characterized by mass spectra steeper than m^{-4} are in energy equipartition, i.e. velocity dispersions scale as $m^{-1/2}$. Such a difference in behaviors is caused by the fact that gravitational stirring and dynamical friction receive major contributions from different parts of planetesimal mass spectra in different cases.

We also consider a possibility that mass distribution has a tail of massive “runaway” bodies sticking out beyond the exponential cutoff of the power-law mass spectrum. We have found that the low mass end of the tail

experiencing dispersion-dominated scattering by all planetesimals exhibits complete energy equipartition: $\sigma_{e,i} \propto m^{-1/2}$. Most massive runaway bodies interact with all planetesimals in the shear-dominated regime, which leads to highly anisotropic velocity distributions of these bodies: $\sigma_e \propto m^{-1/6}$ while $\sigma_i \propto m^{-1/2}$. Time dependence of velocities is determined mainly by the evolution of the cutoff of the power law mass spectrum $m_0 x_c(\tau)$. These asymptotic results derived using analytical means are in good agreement with numerical calculations of planetesimal dynamical evolution presented in §4. They can be easily generalized to cover more complicated planetesimal mass distributions.

Finally, we investigate qualitatively the impact of damping processes such as gas drag or inelastic collisions on the planetesimal disk dynamics. We find that manifestations of these effects are only important for small mass planetesimals; they exhibit themselves in the form of gen-

tle increase of planetesimal random velocities with mass which has been previously observed in “particle in a box” coagulation simulations (Wetherill & Stewart 1993).

Future work in this direction should target the self-consistent coupling of the evolution of planetesimal velocities to the evolution of mass spectrum of planetesimals due to their coagulation. Successful solution of this problem would greatly contribute to our understanding of how terrestrial planets grow out of swarms of planetesimals in protoplanetary disks.

I am indebted to Peter Goldreich for inspiration and valuable advice I have been receiving during all stages of this work. I am also grateful to him and Re'em Sari for careful reading of this manuscript and making a lot of useful suggestions. Financial support of this work by W. M. Keck Foundation is thankfully acknowledged.

APPENDIX

NUMERICAL PROCEDURE.

Evolution of planetesimal eccentricities and inclinations is performed by numerically evolving in time the full system (3) with scattering coefficients smoothly interpolated between shear- and dispersion-dominated regimes. Planetesimals of different masses are distributed in logarithmically spaced mass bins, with bodies in each bin being more massive than planetesimals in previous bin by 1.2. Using numerical orbit integrations we have determined the values of constant coefficients in (9) relevant for the shear-dominated scattering to be

$$B_1 \approx 11.4, \quad B_2 \approx 4.0, \quad D_1 \approx 11.4, \quad D_2 \approx 4.2. \quad (\text{A1})$$

Scattering coefficients in the dispersion-dominated regime are taken from Stewart & Ida (2000) who derived analytical expressions for viscous stirring and dynamical friction rates in the two-body approximation. We translate their results for our gravitational stirring and friction functions $H_{1,2}$ and $K_{1,2}$. This provides us with the dependence of coefficients $A_{1,2}$ and $C_{1,2}$ in (6) on the inclination to eccentricity ratio σ_i/σ_e . Constants $a_{1,2}$ in (7) are fixed to be $a_1 = 1.7, a_2 = 1$.

We assume that mass scale evolves as $x_c(\tau) = F + (\varepsilon\tau)^\chi$, where $F \approx 40$, $\varepsilon = 10^{-4}$, and $\chi = 4$ in the case of shallow mass spectrum with $\alpha = 1.5$ and $\chi = 1.5$ in all other cases. Small parameter ε is introduced to mimic the difference between the timescale of dynamical evolution of planetesimal disk and the timescale of planetesimal growth (which is usually much longer). Besides this, such a form of $x_c(\tau)$ is chosen arbitrarily. Runaway tail is assumed to have a power-law form with the same slope α but much smaller normalization than planetesimal mass distribution. Tail always extends 8 orders of magnitudes beyond x_c to allow interesting velocity regimes to fully develop. Initial distribution of planetesimal eccentricities and inclinations is set to $s(x, 0) = s_z(x, 0) = 3x^{-1/2}$.

VELOCITY EVOLUTION IN A “MIXED” STATE FOR INTERMEDIATE MASS SPECTRUM.

In the case of intermediate mass spectrum runaway bodies with masses x between x_h [defined in (44)] and x_{shear} interact with small planetesimals [less massive than $x_s(x)$ defined by (45)] in the dispersion-dominated regime, but with large ones (heavier than $x_s(x)$) in the shear-dominated regime. As a result, the equations for s and s_z are now hybrid versions of (30) and (35):

$$\frac{\partial s^2}{\partial \tau} = A_1 \int_1^{x_s(x)} dx^* \frac{x^{*2} f(x^*)}{s^{*2}} - 2A_2 s^2 x \int_1^{x_s(x)} dx^* \frac{x^* f(x^*)}{s^{*4}} + \frac{C_1}{x^{2/3}} \int_{x_s(x)}^\infty dx^* x^{*2} f(x^*) - \frac{2C_2 s^2}{x^{1/3}} \int_{x_s(x)}^\infty dx^* x^* f(x^*), \quad (\text{B1})$$

$$\frac{\partial s_z^2}{\partial \tau} = B_1 \int_1^{x_s(x)} dx^* \frac{x^{*2} f(x^*)}{s^{*2}} - 2B_2 s_z^2 x \int_1^{x_s(x)} dx^* \frac{x^* f(x^*)}{s^{*4}} + \frac{D_1}{x^{4/3}} \int_{x_s(x)}^\infty dx^* x^{*2} s^{*2} f(x^*) - \frac{2D_2 s_z^2}{x^{1/3}} \int_{x_s(x)}^\infty dx^* x^* f(x^*) \quad (\text{B2})$$

Following the approach taken in §4.1.2 we neglect l.h.s. of both equations and use (40) and (42) to evaluate integrals in evolution equations. After careful comparison of different contributions in the r.h.s. we find that

$$C_1 \frac{M_2}{x^{2/3}} \approx 2A_2 M_1 \frac{s^2 x}{s_0^4}, \quad (\text{B3})$$

$$B_1 \frac{x_s^{7/2-\alpha}}{s_0^2 x_k^{1/2}} + D_1 \frac{s_0^2 x_k^{1/2}}{x^{4/3}} \int_{\sim x_s}^\infty dx^* (x^*)^{3/2} f(x^*) \approx 2B_2 M_1 \frac{s_z^2 x}{s_0^4}. \quad (\text{B4})$$

Equation (B3) implies that eccentricity stirring of runaway bodies in the mass range $x_h \ll x \ll x_{shear}$ is done mainly by planetesimals with masses $\sim x_c$, for which the interaction proceeds in the *shear*-dominated regime. This heating is balanced by dynamical friction due to the smallest planetesimals, lighter than x_k , which interact with these massive bodies in the *dispersion*-dominated regime.

Vertical heating is somewhat different. Gravitational friction is again dominated by smallest planetesimals which are in the dispersion-dominated mode. Stirring, however, depends on shape of the mass distribution. If $\alpha < 5/2$, second term in the l.h.s. of (B4) — shear-dominated heating by planetesimals with masses between $\sim x_s$ and $\sim x_c$ — dominates⁹ over the first term which represents the effect of dispersion-dominated heating by planetesimals with masses $\sim x_s$. In the opposite case, when $\alpha > 5/2$ both terms in the l.h.s. of (B4) produce roughly equal contributions. Using (B3) & (B4) one can easily derive expressions (46)-(48).

DETAILS OF VELOCITY EVOLUTION FOR THE CASE OF STEEP MASS SPECTRUM.

Substituting our guess (54) into (26) and going through all possibilities appropriate for $\alpha > 3$ we find that self-consistent solutions of power-law type can exist in only two cases:

- Case 1: $3 - \alpha + 2\beta > 0$ & $2 - \alpha + 4\beta > 0$.
- Case 2: $3 - \alpha + 2\beta < 0$ & $2 - \alpha + 4\beta < 0$,

We now consider separately these two possibilities.

Planetesimal velocities.

Case 1.

In this case one can easily see that integrals in the r.h.s. of (26) are mostly contributed by $x^* \sim x$. This allows us to rewrite (26) in the following form:

$$x^{-2\beta} \frac{\partial s_0^2}{\partial \tau} = \frac{x^{3-\alpha+2\beta}}{s_0^2} \int_0^\infty dt \frac{t^{1-\alpha}(1+t)}{1+t^{-2\beta}} \left[\frac{t}{1+t} A_1 - 2 \frac{1}{1+t^{-2\beta}} A_2 \right]. \quad (C1)$$

In arriving at this expression we have used the fact that $f(x, \tau) = x^{-\alpha}$ for $\alpha > 3$ and $1 \ll x \ll x_c$, and extended the integration range over $t \equiv x^*/x$ from 0 to ∞ (because only local region $t \sim 1$ matters). From this equation we can readily see that the l.h.s. of (C1) can be neglected for $x \gg 1$. As a result, a self-consistent power-law solution for s exists only if integral in (C1) is equal to zero. This leads to the following constraint on the required value of β :

$$\frac{I_1(\alpha, \beta)}{I_2(\alpha, \beta)} = \frac{A_1}{2A_2}, \quad I_1(\alpha, \beta) \equiv \int_0^\infty dt \frac{t^{1-\alpha}(1+t)}{(1+t^{-2\beta})^2}, \quad I_2(\alpha, \beta) \equiv \int_0^\infty dt \frac{t^{2-\alpha}}{1+t^{-2\beta}}. \quad (C2)$$

Solving this equation for given α and A_1/A_2 one can find the slope of the mass spectrum $\beta(\alpha, A_1/A_2)$. At a first sight it is not at all clear that equation (C2) should in general possess a solution for β . However, closer look at the problem reveals some interesting patterns.

First of all, it follows from (8) that r.h.s. of (C2) has to be bigger than 1. Second, in the case of energy equipartition $I_1(\alpha, 1/2)/I_2(\alpha, 1/2) = 1$. Third, $I_1(\alpha, \beta) \rightarrow \infty$ as $\beta \rightarrow (\alpha - 2)/4$, while I_2 stays finite. These observations prove that (C2) *always* has a solution for β satisfying the constraint posed by equation (55). Combining restriction (55) with initial constraints of Case 1 we find that Case 1 is only possible for mass spectra with power law slope $3 < \alpha < 4$.

In fact, one can do things even better by considering separately eccentricity and inclination scalings with mass, i.e. using both equations (16). Assuming that the ratio of inclination to eccentricity s_z/s is still constant for $x \lesssim x_c$, one would obtain in addition to (C2) another equation dictated by the inclination evolution. It would be identical to (C2), but with $A_{1,2}$ replaced by $B_{1,2}$. Since both $A_{1,2}$ and $B_{1,2}$ depend only on s_z/s (see §2) one would have two equations for two unknowns: β and s_z/s . Solving them one can uniquely fix both the power law index of planetesimal velocity dependence on mass and the ratio of inclination to eccentricity of planetesimals (which is left undetermined in our simplified analysis of §4).

Case 2.

Restrictions imposed on α and β by the conditions of Case 2 imply that all integrals in the r.h.s. of (26) are dominated by the lower end of their integration range, i.e. by masses ~ 1 . Neglecting time derivative in (26) and balancing contributions in the r.h.s. we find that $\beta = 1/2$ and

$$s(x, \tau) \approx s_0(\tau) x^{-1/2}, \quad x \lesssim x_c. \quad (C3)$$

This solution demonstrates that for $x \gg 1$ our omission of the l.h.s. of (26) is justified for arbitrary behavior of $x_c(\tau)$. It also imposes important restriction on the mass spectra for which this scaling can be realized: α must be bigger than 4. This means that we have found solutions for all possible positive values of α and our study is complete in this sense.

⁹ For $\alpha < 5/2$ integral in (B4) converges at the upper end of its range, near x_c . When $\alpha = 5/2$ this integral is contributed roughly equally by equal logarithmic intervals in mass between $\sim x_s$ and $\sim x_c$; then the second term in the l.h.s. of (B4) dominates over the first one by $\sim \ln(x_c/x_s)$.

Velocities of runaway bodies.

Case 1 ($3 < \alpha < 4$).

Velocity evolution of runaway bodies in the Case 1 is similar to the situation with the intermediate mass spectrum. One finds that when mass x satisfies $x_c \lesssim x \lesssim x_h \equiv s_0^3 x_c^{-3\beta}$ velocity profile is shaped by the dispersion-dominated interaction with *all* small mass planetesimals ($x \lesssim x_c$):

$$s(x, \tau) \approx s_z(x, \tau) \approx \frac{s_0(\tau)}{x^{1/2}} \left(x_c^{1-2\beta} \frac{\tilde{M}_{2+2\beta}}{\tilde{M}_{1+4\beta}} \right)^{1/2}, \quad 3 < \alpha < 4, \quad x_c \lesssim x \lesssim x_h. \quad (\text{C4})$$

The biggest contribution to both stirring and dynamical friction comes the most massive planetesimals with masses $\sim x_c$.

Going to heavier bodies, $x_h \lesssim x \lesssim x_{shear} \equiv s_0^3$, one finds scattering to be in mixed state: some planetesimals [those heavier than $x_s(x) \equiv (s_0/x^{1/3})^{1/\beta}$] interact with big bodies in the shear-dominated regime while the other part (those lighter than x_s) is in the dispersion-dominated regime relative to runaway bodies. It turns out that when $3 < \alpha < 4$ the biggest contributors to both the heating and friction of big bodies are planetesimals of mass $\sim x_s$. Since this is just at the boundary between the shear- and dispersion-dominated regimes, one can expect s_z to behave in the same way as s does [similar to (C4)]. Indeed, we find this to be the case (Figure 8a):

$$s(x, \tau) \approx s_z(x, \tau) \approx \frac{\sqrt{x_s(x)}}{x^{1/6}} \approx \frac{s_0^{1/(2\beta)}}{x^{(1+1/\beta)/6}}, \quad 3 < \alpha < 4, \quad x_h \lesssim x \lesssim x_{shear}. \quad (\text{C5})$$

Runaway bodies with $x \gtrsim x_{shear} \equiv s_0^3 \approx \tau^{3/4}$ experience shear-dominated scattering by smallest planetesimals; using (36) one finds that

$$s(x, \tau) \approx x^{-1/6} \left(\frac{M_2}{M_1} \right)^{1/2}, \quad s_z(x, \tau) \approx s_0(\tau) x^{-1/2}, \quad \alpha > 4, \quad x \gtrsim x_{shear}. \quad (\text{C6})$$

Case 2 ($\alpha > 4$).

We saw in §C.1 that in the Case 2 planetesimal velocity evolution is determined purely by the smallest bodies. As a result, it does not matter whether one studies the dynamics of planetesimals or runaway bodies — all the conclusions of §C.1 stay unchanged as long as the interaction with *smallest* planetesimals occurs in the dispersion-dominated regime. Thus we predict that for $x \lesssim x_{shear}$ velocity spectrum is still given by (C3). Runaway bodies of larger mass, $x \gtrsim x_{shear}$, feel shear-dominated scattering by *all* planetesimals and their velocity dispersions are given by (C6) (exactly like in Case 1).

REFERENCES

- | | |
|---|---|
| <p>Binney, J. & Tremaine, S. 1987, <i>Galactic Dynamics</i>, Princeton University Press, 1987</p> <p>Fermi, E. 1949, Phys. Rev., 73, 1169</p> <p>Greenzweig, Y. & Lissauer, J. J. 1992, Icarus, 100, 440</p> <p>Hayashi, C. 1981, Progr. Theor. Phys. Suppl., 70, 35</p> <p>Hénon, M. & Petit, J. M. 1986, Celestial Mechanics, 38, 67</p> <p>Hornung, P., Pellat, H., & Barge, P. 1985, Icarus, 64, 295</p> <p>Ida, S. 1990, Icarus, 88, 129</p> <p>Ida, S., & Makino, J. 1992, Icarus, 96, 107</p> <p>Ida, S., & Makino, J. 1993, Icarus, 106, 210</p> <p>Inaba, S., Tanaka, H., Nakazawa, K., Wetherill, G. W., & Kokubo, E. 2001, Icarus, 149, 235</p> <p>Kaula, W. M. 1979, Icarus, 40, 262</p> <p>Kenyon, S. J. 2002, PASP, 114, 265</p> <p>Kenyon, S. J. & Luu, J. X. 1998, AJ, 115, 2136</p> <p>Kokubo, E. & Ida, S. 1996, Icarus, 123, 180</p> <p>Kokubo, E. & Ida, S. 2000, Icarus, 143, 15</p> | <p>Makino, J., Fukushige, T., Funato, Y., & Kokubo, E. 1998, New Astronomy, 3, 411</p> <p>Ohtsuki, K. 1999, Icarus, 137, 152</p> <p>Ohtsuki, K., Stewart, G. R. & Ida, S. 2002, Icarus, 155, 436</p> <p>Rafikov, R. R. 2001, AJ, 122, 2713</p> <p>Rafikov, R. R. 2003a, AJ, 125, 906</p> <p>Rafikov, R. R. 2003b, AJ, 125, 922</p> <p>Rafikov, R. R. 2003c, AJ, 125, 942</p> <p>Safronov, V. S. 1972, <i>Evolution of the Protoplanetary Cloud and Formation of the Earth and Planets</i>, NASA TT-F-677</p> <p>Stewart, G. & Ida, S. 2000, Icarus, 143, 28</p> <p>Stewart, G. & Wetherill, G. W. 1988, Icarus, 74, 542</p> <p>Tanaka, H. & Ida, S. 1996, Icarus, 120, 371</p> <p>Wetherill, G. W. & Stewart, G. R. 1989, Icarus, 77, 330</p> <p>Wetherill, G. W. & Stewart, G. R. 1993, Icarus, 106, 190</p> |
|---|---|

TABLE C1. SUMMARY OF ANALYTICAL RESULTS FOR THE VELOCITY SCALING WITH MASS.

Range of α	Mass interval	$\eta = d \ln s / d \ln x$	$\eta_z = d \ln s_z / d \ln x$	Reference
$0 < \alpha < 2$	$x \lesssim x_c$	0	0	Eq. (29)
	$x_c \lesssim x \lesssim x_{shear}$	-1/2	-1/2	Eq. (32)
$2 < \alpha < 3$	$x \lesssim x_{shear}$	-1/6	-1/2	Eq. (37)
	$x \lesssim x_k$	0	0	Eq. (40)
	$x_k \lesssim x \lesssim x_c$	-1/4	-1/4	Eq. (42)
	$x_c \lesssim x \lesssim x_h$	-1/2	-1/2	Eq. (43)
	$x_h \lesssim x \lesssim x_{shear}$	-5/6	-7/6	($\alpha < 5/2$) Eq. (46) & (47)
		-5/6	($4\alpha - 17$)/6 ($\alpha > 5/2$)	Eq. (46) & (48)
$3 < \alpha < 4$	$x \gtrsim x_{shear}$	-1/6	-1/2	Eq. (49)-(51)
	$x \gtrsim x_c$	$-\beta$	$-\beta$	Eq. (C2)
	$x_c \lesssim x \lesssim x_h$	-1/2	-1/2	Eq. (C4)
	$x_h \lesssim x \lesssim x_{shear}$	$-(1 + 1/\beta)/6$	$-(1 + 1/\beta)/6$	Eq. (C5)
	$x \gtrsim x_{shear}$	-1/6	-1/2	Eq. (C6)
$\alpha > 4$	$x \lesssim x_{shear}$	-1/2	-1/2	Eq. (C3), §C.2
	$x \gtrsim x_{shear}$	-1/6	-1/2	§C.2